

PR55 α -controlled protein phosphatase 2A inhibits p16 expression and blocks cellular senescence induction by γ -irradiation

Chitra Palanivel¹, Lepakshe S. V. Madduri¹, Ashley L. Hein², Christopher B. Jenkins¹, Brendan T. Graff¹, Alison L. Camero^{1,3}, Sumin Zhou¹, Charles A. Enke¹, Michel M. Ouellette^{4,5}, Ying Yan^{1,5}

¹Department of Radiation Oncology, University of Nebraska Medical Center, Omaha, NE 68198, USA

²Department of Pathology and Microbiology, University of Nebraska Medical Center, Omaha, NE 68198, USA

³Department of Genetics, Cell Biology, and Anatomy, University of Nebraska Medical Center, Omaha, NE 68198, USA

⁴Department of Internal Medicine - Gastroenterology and Hepatology, University of Nebraska Medical Center, Omaha, NE 68198, USA

⁵Department of Biochemistry and Molecular Biology, University of Nebraska Medical Center, Omaha, NE 68198, USA

Correspondence to: Michel M. Ouellette, Ying Yan; email: mouellet@unmc.edu, yyan@unmc.edu

Keywords: p16, p14, CDKN2A locus, p53, RB, PR55 α , PP2A, γ -irradiation

Received: October 24, 2023

Accepted: February 7, 2024

Published: March 4, 2024

Copyright: © 2024 Palanivel et al. This is an open access article distributed under the terms of the [Creative Commons Attribution License](https://creativecommons.org/licenses/by/4.0/) (CC BY 4.0), which permits unrestricted use, distribution, and reproduction in any medium, provided the original author and source are credited.

ABSTRACT

Cellular senescence is a permanent cell cycle arrest that can be triggered by both internal and external genotoxic stressors, such as telomere dysfunction and DNA damage. The execution of senescence is mainly by two pathways, p16/RB and p53/p21, which lead to CDK4/6 inhibition and RB activation to block cell cycle progression. While the regulation of p53/p21 signaling in response to DNA damage and other insults is well-defined, the regulation of the p16/RB pathway in response to various stressors remains poorly understood. Here, we report a novel function of PR55 α , a regulatory subunit of PP2A Ser/Thr phosphatase, as a potent inhibitor of p16 expression and senescence induction by ionizing radiation (IR), such as γ -rays. The results show that ectopic PR55 α expression in normal pancreatic cells inhibits p16 transcription, increases RB phosphorylation, and blocks IR-induced senescence. Conversely, PR55 α -knockdown by shRNA in pancreatic cancer cells elevates p16 transcription, reduces RB phosphorylation, and triggers senescence induction after IR. Furthermore, this PR55 α function in the regulation of p16 and senescence is p53-independent because it was unaffected by the mutational status of p53. Moreover, PR55 α only affects p16 expression but not p14 (ARF) expression, which is also transcribed from the same *CDKN2A* locus but from an alternative promoter. In normal human tissues, levels of p16 and PR55 α proteins were inversely correlated and mutually exclusive. Collectively, these results describe a novel function of PR55 α /PP2A in blocking p16/RB signaling and IR-induced cellular senescence.

INTRODUCTION

Senescence in normal cells is a permanent cell cycle arrest that can be triggered in response to various intrinsic and extrinsic genotoxic stressors, such as telomere dysfunction, oxidative stress, and DNA

damage [1, 2]. Irrespective of the stimulus, senescent cells become permanently arrested in the G1 phase and this arrest is accompanied by alterations in phenotypic properties and gene expression. Among these changes, the induction of senescence-associated β -galactosidase (SA- β -gal) activity is the hallmark of senescent cells

[3]. Senescence induction is mainly executed by one of two distinct pathways or by both: the p16 pathway that inhibits the CDK4/6 kinases and the p53/p21 pathway that inhibits the CDK2 kinase [4–6] (Figure 1). Both CDK4/6 and CDK2 activities are essential for cells to progress through the G1/S transition of the cell cycle and initiate DNA replication in the S-phase [7]. The inhibition of CDKs by p16 and/or p21 results in the hypo-phosphorylation and activation of the RB protein, which subsequently blocks cell cycle progression. While in some circumstances there is crosstalk between the p53/p21 and p16 pathways,

the two pathways operate independently and can be activated separately [8, 9].

The expression of p16 and p21 is primarily regulated at the mRNA level. The up-regulation of p21 observed at senescence is induced by p53 [10], whereas the up-regulation of p16 is more complex and involves multiple mechanisms, most of which remain poorly understood. The p16 protein is encoded by the *CDKN2A* locus, which also encodes for the p14 protein (also known as ARF), an upstream activator of p53. In young and unstressed cells, the *CDKN2A* locus is

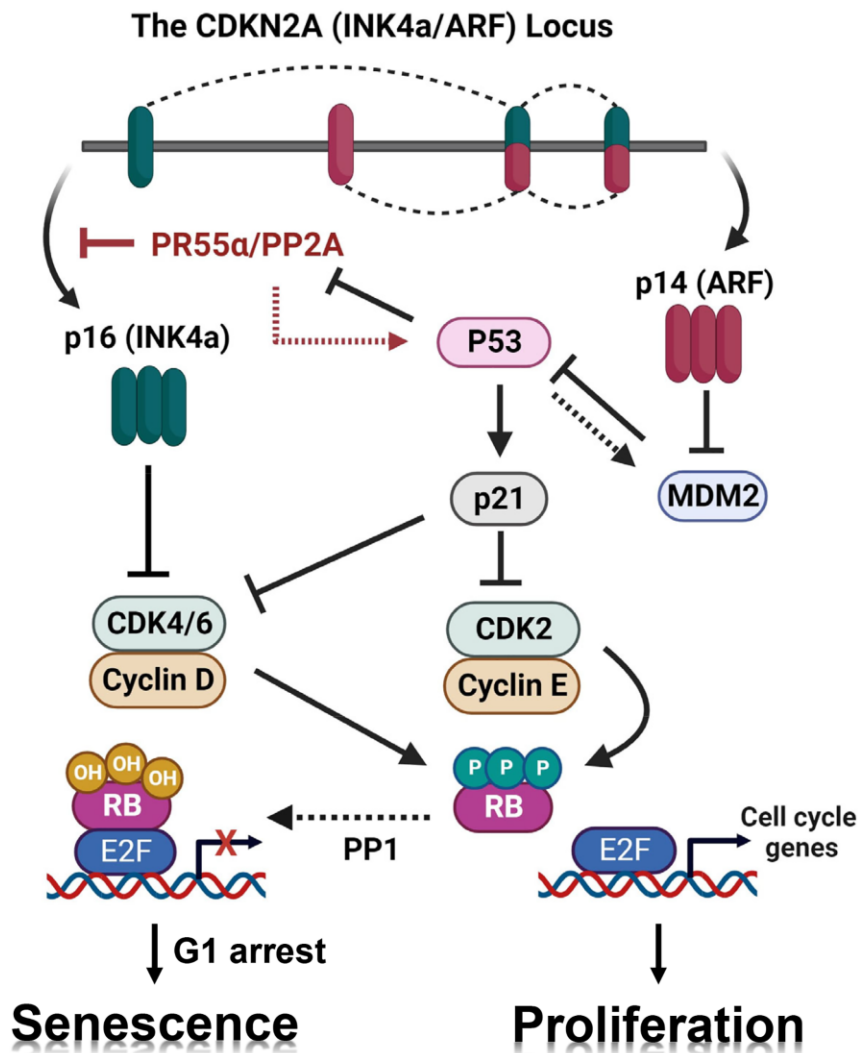


Figure 1. Working model for the regulation of the p16/RB pathway and senescence induction by PR55α. Black lines depict our current understanding of the respective roles of the p16/RB and p53/p21 pathways in the promotion of cellular senescence in response to genotoxic stressors [83, 84]. The *CDKN2A* locus produces both the p16 (INK4a) and p14 (ARF) proteins using both separate promoters and alternative splicing. The p16 protein blocks the CDK4/6 kinases leading to RB activation, which is required for G1 cell cycle arrest and senescence induction. The p14 protein stabilizes p53 by inhibiting the MDM2 E3 ubiquitin ligase, resulting in p21 (a p53 target gene) induction and subsequent inhibition of CDK2 and CDK4/6, which also leads to RB activation that promotes G1 cell cycle arrest and senescence. We have previously reported that p53 negatively regulates PR55α protein stability [28]. However, the p53 mutational status had no detectable impact on the effects of PR55α on the expression of p16 and induction of senescence by IR. Red lines depict novel findings presented in this report: (1) PR55α-controlled PP2A enhances IR-induced p53/p21 signaling and (2) PR55α inhibits p16 transcription independently of p53 function.

maintained in an epigenetically repressed state by PcG protein complexes and the repressive histone marks that they generate (H3K27me3, H2AK119Ub) [11]. The expression of p16 requires alterations in PcG function and recruitment of transcription factors and other epigenetic regulators, such as the DDB1/CUL4-MML1 complex. In addition, p16 mRNA expression can be regulated at the post-transcriptional level. When cells undergo replicative senescence, the p16 mRNA becomes stabilized and this requires elements located in its 3'-untranslated region (3'-UTR) and 5'-UTR [12, 13]. The AU-rich element-binding factor 1 (AUF1), also called heterogeneous nuclear ribonucleoprotein D (hnRNP D), is a well-characterized RNA-binding protein that recognizes adenylate/uridylylate-rich elements known to control the stability of mRNA transcripts [14]. The AUF1/hnRNP D locus (hereafter referred to as AUF1) produces transcripts encoding four isoforms (p37, p40, p42, and p45), which differ slightly in their RNA-binding abilities [15]. With other subunits, AUF1 is part of a large complex that destabilizes mRNAs carrying AU-rich elements in their 5'-UTR or 3'-UTR, as in the case of the p16 mRNA, where the binding of AUF1 leads to rapid mRNA decay [16].

The *CDKN2A* locus on chromosome 9p21, a region that encodes both p16 and p14, is frequently deleted or otherwise altered in cancers. The p16 and p14 mRNAs are both made of three exons, the second and third of which are shared between the two [17]. To produce two entirely different proteins from the same locus, the two mRNA are transcribed from separate promoters and read their common exons in different frames (Figure 1). Functionally, p16 inhibits CDK4/6, which then blocks the G1/S transition by preventing the phosphorylation and inactivation of RB, while p14 activates p53 by inhibiting MDM2, which acts as an E3 ubiquitin ligase that targets p53 for degradation [18]. At senescence, the p16 and p14 proteins can be induced together or just p16 alone, depending on the conditions, the cell type, or the species. Through their respective regulation of the RB and p53 pathways, p16 and p14 proteins serve as key regulators of both the cell cycle and cellular senescence [19].

Protein phosphatase 2A (PP2A) is a family of heterotrimeric holoenzyme complexes that constitute the majority of Ser/Thr phosphatase activities in human cells [20]. Each PP2A trimer consists of a catalytic subunit, a scaffold subunit, and a regulatory subunit. While both the catalytic and scaffold subunits are each produced as two highly conserved isoforms, the regulatory subunit comes in 27 different isoforms, with each dictating the substrate specificity and cellular localization of the associated holoenzyme [21]. PR55 α is a PP2A regulatory subunit and PR55 α -controlled

PP2A complexes have been shown to regulate proteins involved in cell cycle control and response to various genotoxic stress, including DNA damage and nutrient deprivation [22]. Several reports, including ours, have shown that PR55 α -controlled PP2A promotes the activation of oncogenic pathways by dephosphorylating inhibitory phosphorylation sites on key regulators of the cell cycle, including ERK1/2, β -catenin, c-Myc, and Yes-associated protein (YAP) [23–26]. Consistently, our studies have shown that PR55 α supports oncogenic transformation and the malignant phenotype of pancreatic cancer cells [23, 27, 28]. In a recent report, we discovered that the protein stability of PR55 α is regulated by the E3 ubiquitin ligase FBXL20 [28], a gene known to be up-regulated by the transcriptional activity of p53 [29]. Since oncogenesis and senescence are mutually exclusive events and PR55 α promotes oncogenic transformation, we investigated the impacts of PR55 α expression on the induction of premature senescence by ionizing radiation (IR). The results of this study reveal an essential role for PR55 α -controlled PP2A as a potent inhibitor of p16 expression and induction of senescence by IR. The data also indicate that this function of PR55 α is p53 independent since it is also observed in p53 mutant cancer cells.

RESULTS

PR55 α inhibits the expression of p16 in human pancreatic normal and cancer cells

The p16 tumor suppressor is a major CDK4/6 inhibitor that plays an essential role in the induction of cellular senescence [30]. The loss of p16 occurs in >90% of pancreatic cancer and has been identified as a driver mutation in pancreatic cancer tumorigenesis [31]. We have previously reported an essential role for PR55 α in maintaining the tumorigenicity and metastatic potential of human pancreatic cancer cells [23, 27]. Here, we assessed the impacts of PR55 α on the expression and function of p16 in both HPNE cells and CD18/HPAF cells. HPNE cells are human normal pancreatic ductal cells that we previously immortalized with telomerase [32, 33]. CD18/HPAF cells are human pancreatic cancer cells driven by the KRAS oncogene and mutant p53^{P151S} [34].

Through retroviral transductions, stable lines of normal HPNE cells were engineered to express a Dox-inducible PR55 α , while stable lines of CD18/HPAF cells were engineered to express a Dox-inducible PR55 α -shRNA. Since p16 plays an essential role in most forms of cellular senescence, from replicative senescence to stress-induced premature senescence, we assessed the effects of PR55 α on p16 expression and premature senescence-induced by IR in the context of both normal cells and cancer cells of the pancreas. To induce senescence in these experiments,

we have used a high dose of radiation (10 Gy), similar to doses used in extreme hypofractionation radiation therapy, now made possible by advances in stereotactic radiotherapy [35, 36]. In radioresistant forms of cancer, such as pancreatic cancer, this approach may be producing better outcomes.

In the normal HPNE cells, PR55 α induction abolished the expression of p16 (Figure 2A). After exposure to γ -irradiation, p16 expression was slightly increased in both the control and PR55 α -overexpressing HPNE cells. However, the magnitude of the minor increase of p16 induced by IR was the same in the control cells and PR55 α -overexpressing cells (Figure 2A). For validation, we tested the effect of PR55 α on p16 expression in CD18/HPAF pancreatic cancer cells, which harbor a p53^{P152S} mutant thus lacking a functional p53/p21 pathway [34]. Although CD18/HPAF cells express a p16 protein that contains an in-frame deletion from amino acids (aa) 29 to 34 [37], this mutation does not appear to affect p16 mRNA stability, protein expression, or even p16 function since it does not interfere with the ability of p16 to bind and inhibit CDK4/6, a function mediated by its Ankyrin repeats AR2 (aa 36–69) and AR3 (aa 70–100)

[38]. As predicted, the knockdown of PR55 α by shRNA in CD18/HPAF cells resulted in the opposite effect compared to the overexpression of PR55 α in the normal HPNE cells. Again, the high levels of PR55 α expression were associated with low levels of p16 (Figure 2B). IR exposure also resulted in a subtle increase in p16 levels in CD18/HPAF cells over time, but the magnitude of this induction was the same in the control and PR55 α -knockdown cells (Figure 2B). It was also noticed that there was a transient increase of the p16 level in control cells at 2 hours following IR. The cause of the effect is unknown, which could be due to a temporary increase in the protein stability of p16 prompted by IR-activated stress signaling.

Because p14 and p16 are essentially transcribed from the *CDKN2A* locus, albeit from distinct promoters (Figure 1), we assessed the effects of PR55 α on p14 expression after IR. In both the HPNE and CD18/HPAF cells, the manipulation of PR55 α levels did not result in a similar effect on p14 as it did on p16. In the HPNE cells, for example, PR55 α overexpression abolished p16 expression but it slightly increased p14 levels. These results show that PR55 α specifically inhibits p16 expression but not p14 expression.

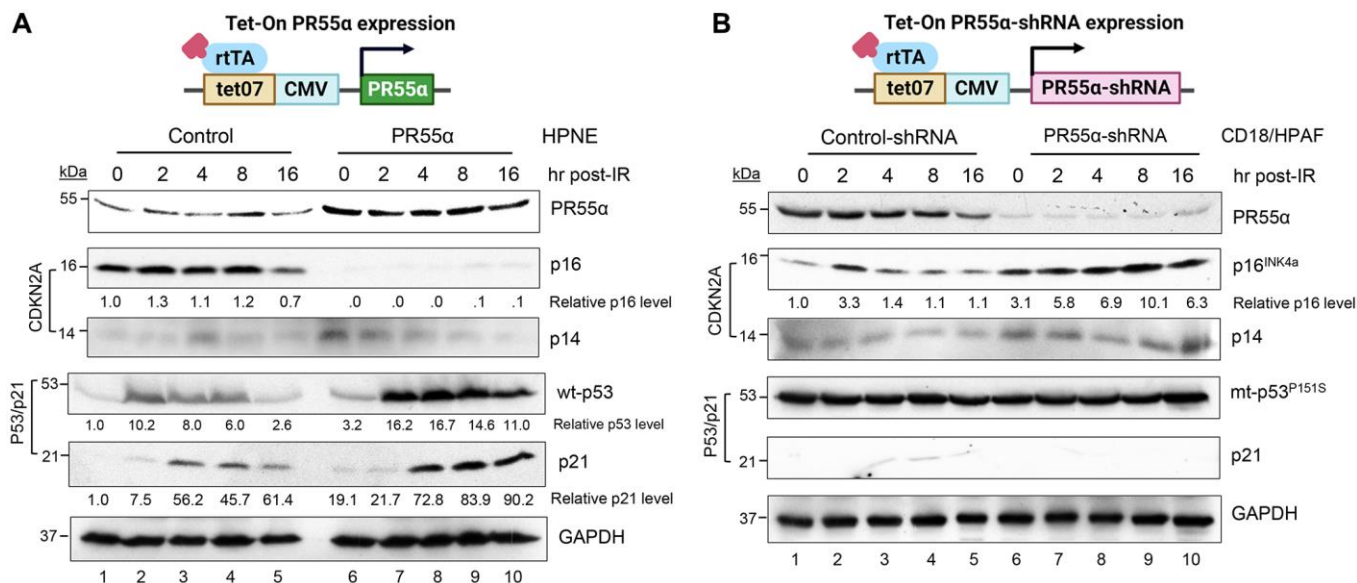


Figure 2. PR55 α suppresses p16 protein expression in normal and cancer cells originating from the human exocrine pancreas.

(A) Human pancreatic normal ductal (HPNE) cells were stably transduced with a retroviral vector expressing a Dox-inducible PR55 α cDNA (PR55 α). As a control, HPNE cells stably transduced with a relevant empty retroviral vector were included in the analysis (Control). Following the induction of ectopic PR55 α expression by Dox (1 μ g/ml) for 2 days, cells were exposed to 10 Gy of ionizing radiation (IR), incubated for the indicated hours, and analyzed by immunoblotting for the levels of p16, p14, p53, and p21. GAPDH in the lysates was measured as an internal control. (B) Human pancreatic ductal adenocarcinoma cells (CD18/HPAF) were stably transduced with a lentiviral vector expressing a Dox-inducible shRNA against either PR55 α (PR55 α -shRNA) or an irrelevant negative control (Control-shRNA). Following induction of the shRNA with Dox (2 μ g/ml) for 5 days, the cells were exposed to 10 Gy IR, incubated for the indicated hours, and analyzed by immunoblotting for the levels of the indicated proteins. GAPDH in the lysates was again used as an internal control. The difference in the p16 levels between HPNE-Control and HPNE-PR55 α cells, as well as between the CD18/HPAF-Control-shRNA and CD18/HPAF-PR55 α -shRNA cells were determined to be statistically significant (HPNE-Control vs. HPNE-PR55 α , $p < 0.001$; CD18/HPAF-Control-shRNA vs. CD18/HPAF-PR55 α -shRNA, $p = 0.004$).

PR55 α enhances the response of the p53/p21 pathway to IR exposure

The p53/p21 pathway plays a key role in DNA damage-induced cell cycle checkpoint response and senescence induction [39]. Loss of p53 function via mutations is the most frequent event occurring across all cancer types and is a main driver of pancreatic cancer development and progression [40]. We previously reported on the role of p53 as a negative regulator of the protein stability of PR55 α , whose function supports several oncogenic pathways, including ERK, β -catenin, c-Myc, and YAP [23–28]. Since p53's role as a tumor suppressor counteracts that of PR55 α in the promotion of oncogenic pathways, we examined the impacts of PR55 α on the response of the p53/p21 pathway to IR.

As shown in Figure 2A, ectopic PR55 α expression in HPNE cells caused a 3.2-fold elevation in the steady-state level of p53, as well as markedly enhanced p53 induction by IR in HPNE cells. Within 2 h post-IR, p53 was induced in both the HPNE/control and HPNE/PR55 α cells, but the induction was 6–8 fold higher in the latter (Figure 2A). To validate these results, we assessed the effects of PR55 α on p21 expression, which is known to be induced by the transcriptional activity of p53 [41]. Consistently, ectopic PR55 α expression in HPNE cells led to higher steady-state levels of p21, which is in line with its effect on p53 (Figure 2A). Like p53 levels, p21 levels were also induced by IR, albeit with a kinetic that was delayed by 2 hours compared to the induction of p53 (Figure 2A). Similar to p53, the magnitude of the induction of p21 by IR was higher in HPNE/PR55 α cells compared to the HPNE/control cells (Figure 2A).

For comparison, we assessed the effect of PR55 α level on mutant p53 expression in CD18/HPAF pancreatic cancer cells. The mutant p53 expressed in CD18/HPAF cells harbors a P151S mutation in the DNA binding domain of p53, thus abolishing its activity as a transcription factor [34]. As shown in Figure 2B, the knockdown of PR55 α by shRNA did not affect the level of the p53^{P151S} mutant protein, either in the presence or absence of IR (Figure 2B), which was in contrast to the situation observed in HPNE cells known to express wild-type (wt) p53 protein (Figure 2A). In agreement with the lack of functional p53 in CD18/HPAF cells, levels of p21 were extremely low in these cells and were not particularly affected by either the knockdown of PR55 α or exposure to IR (Figure 2B). These results indicate that PR55 α only increases the expression of wt-p53, but not mutant p53. Taken together with our analyses of *CDKN2A* gene products, these results show that PR55 α inhibits p16 expression while simultaneously enhancing the expression of wt p53. However, this

enhancement of p53 expression is not associated with changes in p14 levels and is thus independent of p14.

PR55 α suppresses p16 expression by inhibiting its mRNA transcription

To define the mechanism by which PR55 α inhibits p16 expression, we first examined the impacts of PR55 α on the protein stability of p16 using the cycloheximide (CHX)-chase assay, as described in our previous work [28]. CD18/HPAF cells expressing the control- or PR55 α -shRNA were incubated with 15 μ g/ml cycloheximide to block protein synthesis to allow measurements of p16 protein decay. As depicted in Figure 3A, PR55 α knockdown by shRNA did not result in a significant change in the p16 protein half-life in CD18/HPAF cells, indicating a lack of effect of PR55 α on the p16 protein decay process.

We next assessed the effects of PR55 α on p16 mRNA expression using real-time quantitative Reverse Transcription and PCR (qRT-PCR). As shown in Figure 3B, the p16 mRNA level was decreased by ~70% in the HPNE cells expressing ectopic PR55 α compared to the control HPNE cells. Conversely, the PR55 α knockdown by shRNA resulted in a 3–5 fold induction in p16 mRNA level in CD18/HPAF cells compared to the control cells (Figure 3B). Statistically, these changes were all determined to be highly significant. To further define the mechanism by which PR55 α reduces p16 mRNA expression, we analyzed the impact of PR55 α on p16 promoter activity using a luciferase reporter assay. HPNE and CD18/HPAF cells were transiently co-transfected with two reporter vectors: a vector expressing firefly luciferase under the control of the p16 promoter (nucleotides –3243 to –165) and a control vector expressing Renilla luciferase from the SV40 promoter (Figure 3C). As shown in Figure 3C, ectopic PR55 α expression in HPNE normal cells resulted in >90% inhibition of the p16 promoter activity compared to the control cells. Conversely, shRNA knockdown of PR55 α in CD18/HPAF cancer cells resulted in approximately 85-fold induction in the p16 promoter activity. Together, these results indicate that the inhibition of p16 expression by PR55 α is at least in part mediated by the repression of its promoter activity.

Knocking down AUF1 does not affect the inhibition of p16 expression by PR55 α

AUF1 is an RNA-binding protein that has been reported to promote p16 mRNA decay during replicative senescence [13]. Thus, we examined the effect of AUF1 on the suppression of p16 expression by PR55 α . AUF1 was knocked down by siRNA in both HPNE control

and PR55 α overexpressing cells and the resulting cells were analyzed for differences in the levels of AUF1 and p16 after 48 h incubation. In HPNE control cells, the knockdown of AUF1 resulted in a 6-fold induction of p16 protein expression (Figure 3D), which is consistent with previous findings [13]. However, in the PR55 α overexpressing cells, the knockdown of AUF1 did not suffice to reallocate the expression of the p16 protein (Figure 3D). Thus, the AUF1-mediated mRNA decay mechanism is not responsible for the inhibition of p16 expression by PR55 α .

PR55 α promotes RB phosphorylation

RB plays a key role in the induction of both replicative senescence and stress-induced premature senescence, both of which are known to exhibit a permanent cell cycle arrest at the G1 phase caused by the sequestration of the E2F transcription factor by RB [42–44]. During cell proliferation, RB is phosphorylated by CDK4/6 and then CDK2 kinases, which free E2F to induce the transcription of genes needed for the S phase [45]. In senescent cells, CDK4/6 and CDK2 are permanently

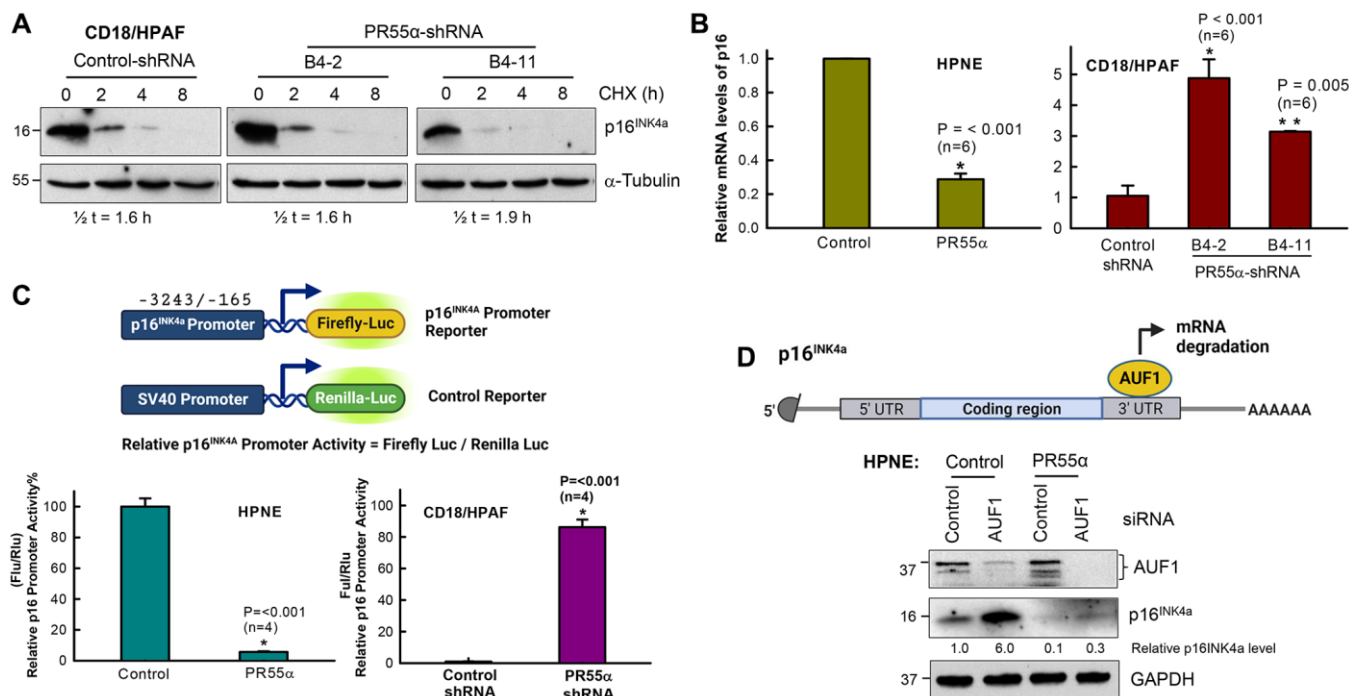


Figure 3. PR55 α inhibits p16 expression by suppressing its mRNA transcription. (A) PR55 α does not affect p16 protein stability. CD18/HPAF cells stably transduced with Dox-inducible PR55 α -shRNA or Control-shRNA were cultivated in media containing 2 μ g/ml Dox for 5 days to induce the shRNA, after which cells were exposed to cycloheximide (CHX, 15 μ g/ml) to halt protein synthesis. Cell lysates collected at the indicated time points after CHX addition were analyzed for changes in p16 protein levels. The α -tubulin protein has a long half-life and was used as an internal control. Relative p16 protein levels were determined after normalization with the α -tubulin levels and these normalized values were used to calculate the protein half-life of p16. Half-lives were estimated by linear regression analysis of p16 normalized levels against time using SigmaPlot. (B) PR55 α inhibits p16 mRNA expression. Left panel: HPNE expressing the Dox-inducible PR55 α (HPNE/PR55 α), or empty vector (HPNE/Control) was treated with Dox (1 μ g/ml) for 3 days. Right panel: CD18/HPAF cells expressing the Dox-inducible PR55 α shRNA (B4-2, B4-11) or Control shRNA (Control) were treated with Dox (2 μ g/ml) for 5 days. At the end of each treatment, RNA was isolated and analyzed by quantitative RT-PCR for differences in p16 mRNA. The relative abundance of the p16 mRNA was calculated by normalizing the p16 mRNA levels with those of the GAPDH mRNA, with the data represented as mean \pm S.D. (bar graphs). Statistical significance was calculated by a Student's *t*-test (HPNE cells) or one-way ANOVA (CD18/HPAF). The difference with the Control group ($n = 6$ /group) was determined to be statistically significant at $*p < 0.001$ or $**p < 0.005$. (C) PR55 α suppresses p16 promoter activity. HPNE and CD18/HPAF cells in the presence/absence of ectopic PR55 α and PR55 α -shRNA expression, respectively, were co-transfected with a Firefly luciferase reporter under the control of the p16 promoter and a control Renilla luciferase reporter driven by the SV40 promoter. Two days after transfection, Firefly, and Renilla luciferase activities were measured separately in each lysate, as described in the Materials and Methods. p16 promoter activity was calculated by normalizing the activity of Firefly luciferase over that of Renilla luciferase. The graphs show relative p16 promoter activities in the indicated cell samples and are expressed as the mean \pm S.D. of two independent experiments done in duplicates. *Statistically significant in a Student's *t*-test with $p < 0.001$. (D) HPNE/Control and HPNE/PR55 α cells were incubated in the presence of 1 μ g/ml Dox for 48 h to induce PR55 α expression, after which cells were transfected with either a non-targeting siRNA (Control) or AUF1 siRNA. Two days later, cells were analyzed by immunoblotting for differences in levels of AUF1 and p16. GAPDH was used as an internal standard. The levels of p16 and GAPDH were quantified using Fiji-ImageJ software and relative p16 levels in the samples were determined after normalizing it with GAPDH levels.

inhibited by the induction of the p16 and p21 proteins, respectively [46] (Figure 1). Since PR55 α affected the expression of both p16 and p21 but in different ways (Figure 2), we investigated the net effect of PR55 α on RB phosphorylation.

Consistent with the preponderant role played by p16 in cellular senescence [47], the effects of PR55 α on RB phosphorylation mirrored those observed with the p16 protein in both the normal and cancer cells. In HPNE cells, where PR55 α overexpression suppresses p16 expression (Figure 2A, lane 6 vs. 1), the phosphorylation of RB-Ser780 (Figure 4A, lane 6 vs. 1) was elevated, indicative of increased CDK4/6 kinase activity [48, 49]. Similar to the situation observed with p16 in the HPNE/PR55 α cells (Figure 2A), IR only had minor impacts on the Ser780 phosphorylation of RB, which remained high across all time points post-IR (Figure 4A).

For validation, we examined the effect of PR55 α on RB phosphorylation in CD18/HPAF pancreatic cancer cells. The knockdown of PR55 α resulted in a

~50% decrease in the steady-state phosphorylation of RB-Ser780 in the log-phase CD18/HPAF cells (Figure 4B, lane 6 vs. 1), which is consistent with the elevated p16 levels in these cells relative to the control cells (Figure 2B, lane 6 vs. 1). Furthermore, IR exposure of control CD18/HPAF cells resulted in the induction in RB-Ser780 phosphorylation, whereas IR exposure of PR55 α -knockdown CD18/HPAF cells rather resulted in a time-dependent decrease in RB-Ser780 phosphorylation (Figure 4B). Together, these results support a role for PR55 α in the suppression of p16/RB signaling (Figure 4C).

PR55 α impedes the cell cycle response of pancreatic normal and cancer cells to IR exposure

In response to DNA damage, cells elicit a cell cycle checkpoint response, leading to either cell cycle arrest for DNA repair, or replicative cell death (apoptosis or else senescence) if the damage is irreversible [50, 51]. Normal cells possess wild-type p53, which can be rapidly activated by DNA damage to induce p21

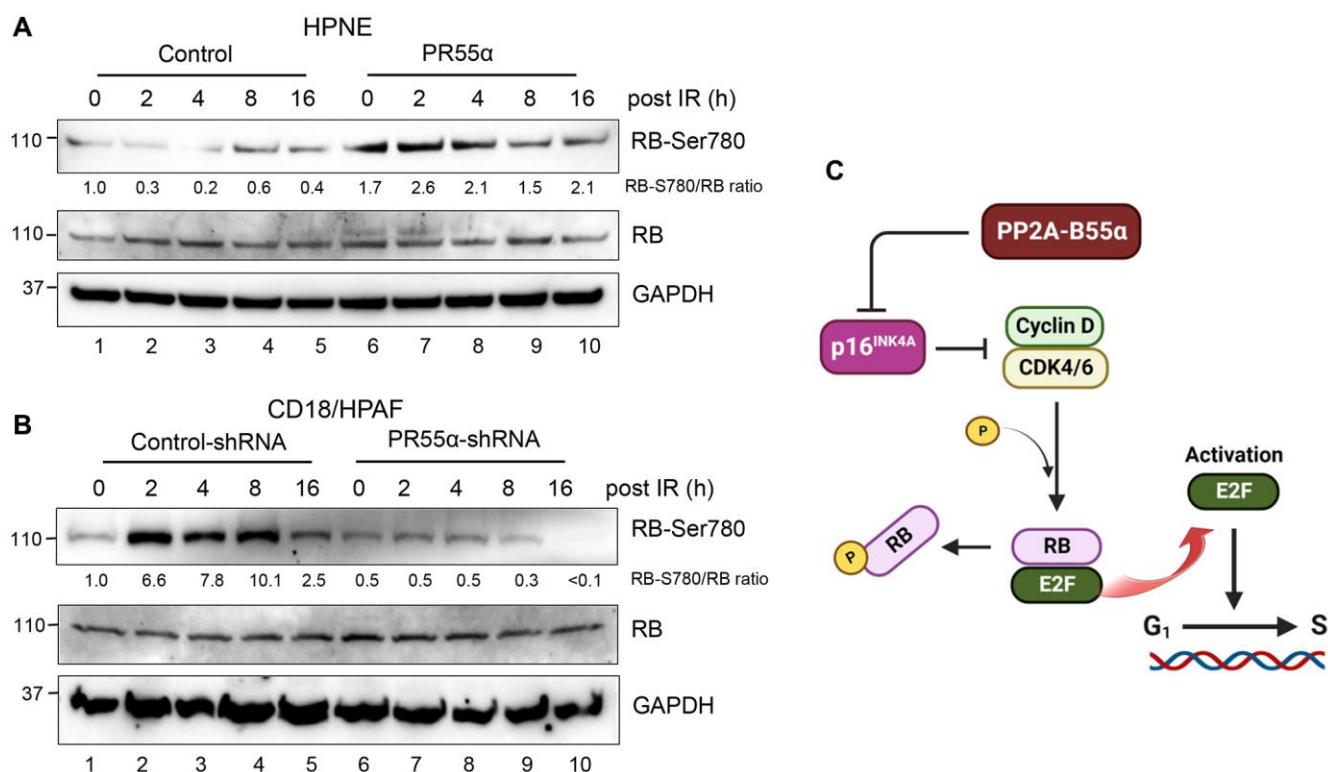


Figure 4. PR55 α expression increases RB phosphorylation in normal and malignant pancreatic cells. (A) A schematic depiction of the regulation of the p16/RB cascade by PR55 α -controlled PP2A enzymes. PR55 α suppresses the expression of p16, which acts as the primary inhibitor of the CDK4/6 kinases that phosphorylate and inactivate RB, thereby resulting in its dissociation from the E2F transcriptional factor. The net effect of PR55 α is promoting the G1/S transition by allowing the phosphorylation of RB and the release of E2F. (B) HPNE cells transduced with Dox-inducible PR55 α , or control vector were incubated with 1 μ g/ml Dox for 3 days to induce ectopic PR55 α expression. The cells were exposed to 10 Gy IR and then incubated for the times indicated. Harvested cells were analyzed for RB-Ser780 phosphorylation, total RB level, and GAPDH (as an internal control). (C) CD18/HPAF-transduced with the Control or PR55 α shRNA were incubated with 2 μ g/ml Dox for 5 days to knockdown PR55 α expression, after which cells were analyzed by immunoblotting for differences in RB-Ser780 phosphorylation, total RB, and GAPDH.

expression and arrest the cell cycle at the G1 phase while promoting DNA repair [52]. However, most cancer cells harbor p53 mutations and are thus defective in the G1 checkpoint that requires the p53/p21 pathway. In these cancer cells, DNA damage only activates the G2 checkpoint, thereby blocking the G2/M transition to allow DNA repair [53]. Yet, both the G1 and G2 checkpoints are dependent on the activation of RB to block cell cycle progression and this activation can be triggered by either the p53/p21 pathway and/or the p16/RB pathway (Figure 1) [8]. Because PR55 α inhibits p16 expression in both the normal HPNE cells expressing wild-type p53 and the CD18/HPAF cancer cells expressing mutant p53, we decided to examine the impacts of PR55 α on the IR-induced cell cycle response. For this purpose, exponentially proliferating HPNE and CD18/HPAF cells, with/without PR55 α manipulations, were exposed to increased doses of IR and analyzed 24 hours later for changes in DNA content by Fluorescence-activated cell sorting (FACS).

As shown in Figure 5, IR exposure of HPNE/Control cells resulted in a small but statistically significant increase in the percent cells in the G1 phase ($p = 0.016$), which was accompanied by a concurrent decrease in

cells in the S phase ($p = 0.021$) and little change in the cells at the G2/M phases, all indicative of a G1 cell cycle arrest. In contrast, in PR55 α -overexpressed HPNE cells (HPNE/PR55 α), IR exposure produced little, if any, effects on the cell cycle profile compared to the unirradiated cells (Figure 5). Because HPNE/Control cells express both wild-type p53 and wild-type p16, their cell cycle response to IR was controlled by the combined activities of the p53/p21 and p16/RB pathways. In contrast, in HPNE/PR55 α cells, since the expression of p16 was inhibited to near totality while the p53/p21 was further enhanced (Figure 2A), the effect of IR on the cell cycle response of these cells could only be attributed to the p53/p21 pathway.

Next, we examined the effect of PR55 α on the cell cycle response of CD18/HPAF cells, which express the p53^{P151S} mutant along with very low levels of p16 [37, 54], making these cells deficient in both p53 and p16 functions and lacking a functional G1 cell cycle checkpoint as part of their DNA damage response [53, 55]. However, CD18/HPAF cells still possess an intact G2 checkpoint as part of their DNA damage response, which can function independently of p53 and p16 [56, 57]. As shown in Figure 5, IR exposure of

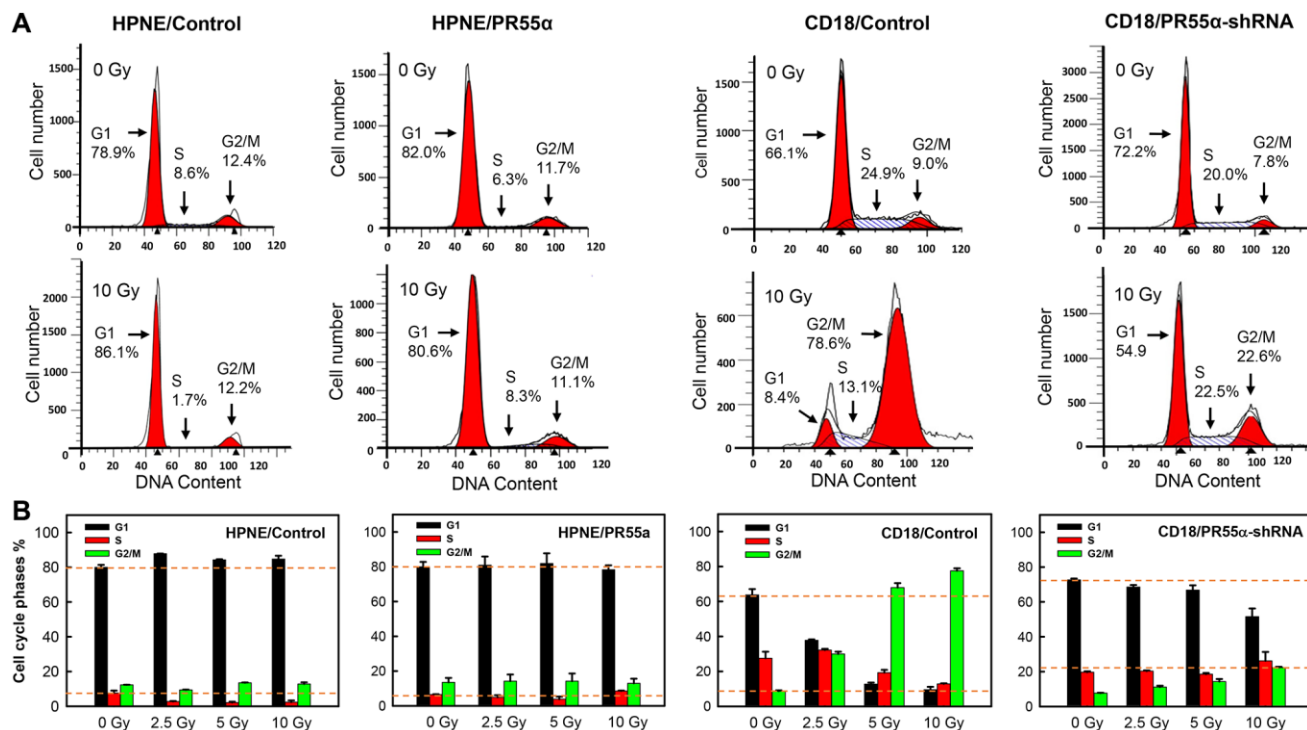


Figure 5. Effect of PR55 α on the cell cycle response of normal and cancer cells to IR. Log-phase growing HPNE (Control- or PR55 α -transduced) and CD18/HPAF cells (Control-shRNA or PR55 α -shRNA transduced) were incubated in media containing 1 μ g/ml Dox for 3 days and 2 μ g/ml Dox for 5 days, respectively, to manipulate PR55 α expression. The cells were exposed to IR at indicated doses, incubated for 24 hours, and then stained with propidium iodide (PI) and analyzed for DNA content using FACS. (A) Representative FACS analyses are shown. The location and percent of cells in the G1, S, and G2/M phases of the cell cycle are indicated by arrows. (B) Bar graphs depicting the percent cells in the G1, S, and G2/M phases of the cell cycle. Each bar represents the mean \pm S.D. of two separate experiments, each done in duplicates.

CD18/HPAF control cells (*CD18/Control*) resulted in dose-dependent increases in cells at the G2/M phases that were accompanied by concurrent diminutions in percent cells at the G1 and S phases, which is indicative of a G2/M cell cycle arrest. In the PR55 α knockdown cells (*CD18/PR55 α -shRNA*), while IR still led to a G2/M cell cycle arrest (Figure 5), the percent cells arrested at the G2/M phases was much reduced compared to the irradiated control cells (*CD18/Control*), by more than a factor of 3 (22.6% versus 78.6%). In the PR55 α knockdown cells, IR also did not substantially deplete the percent cells in the G1 or S phases of the cell cycle. Compared to only 8.4% of CD18/Control cells that were retained in the G1 phase after IR, 54.9% of CD18/PR55 α -shRNA were still detected in the G1 phase after IR, which corresponds to a 6.5-fold difference in the percent cells in the G1 phase between the two isogenic cell populations (Figure 5). Collectively, these results indicate that, although the parental CD18/HPAF cancer cells lack a functional G1 checkpoint and thus instead respond to IR with the induction of a G2/M cell cycle arrest, the knockdown of PR55 α by shRNA was sufficient to induce high levels of p16 expression, which may have then allowed the bulk of the cells to remain in G1 after IR. These results from CD18/HPAF cells are again consistent with the negative regulation of p16 expression by PR55 α and subsequent impacts on RB phosphorylation and cell cycle checkpoints.

PR55 α inhibits p16-dependent cellular senescence induction by IR

Our findings in Figures 2–5 reveal PR55 α -controlled PP2A as a potent inhibitor of p16 expression and G1 checkpoint activation. In normal human cells, activation of the G1 checkpoint by genotoxic assaults is required for the induction of cellular senescence, both replicative and premature [7, 13, 58], to prevent the damaged cells from dividing and subsequently becoming malignant [59–61]. The induction of senescence commonly involves two key regulators: the p16/RB and/or p53/p21 pathways, depending on the insult and the cell type [4–6, 58]. To examine the effects of PR55 α on senescence induction by IR, we measured the activity of senescence-associated β -galactosidase (SA- β -gal), a hallmark of senescent cells [62]. In control HPNE cells, SA- β -gal activity was undetectable before IR exposure (0 Gy) but detected in ~60% and ~80% of cells after exposure to a single (7 Gy) or double (2×7 Gy) doses of IR, respectively. In contrast, PR55 α overexpression in HPNE cells markedly diminished senescence induction by IR, with less than 10% of irradiated HPNE/PR55 α cells staining positive for SA- β -gal activity after either the 1×7 Gy or 2×7 Gy treatment (Figure 6A). Likewise, while

control CD18/HPAF cells exposed to 7 Gy IR only exhibited <1% SA- β -gal positive cells at 7 days post-IR, < 90% of irradiated PR55 α -knockdown CD18/HPAF cells were positive for SA- β -gal activity post-IR (Figure 6B). Senescent HPNE or CD18/HPAF cells were also typically larger and flatter in shape compared to their respective unirradiated controls (Figures 6A, 6C). Collectively, in either p53-wt HPNE normal cells or p53-mutant CD18/HPAF cancer cells, senescence induction in response to IR requires a low level of PR55 α expression, thereby revealing PR55 α as a potent inhibitor of IR-induced cellular senescence. Also, this regulation of p16 expression by PR55 α was independent of the p53/p21 pathway, since the IR-activated p53/p21 cascade was further enhanced by the overexpression of PR55 α in HPNE/PR55 α cells, in which IR still failed to induce senescence. Conversely, despite CD18/HPAF cells harboring a mutant p53, the knockdown of PR55 α still resulted in increased p16 expression and induction of senescence in response to IR exposure (Figures 2 and 6).

To confirm that p16 expression is required for senescence induction by IR in PR55 α knockdown cells, we utilized the AsPC-1 pancreatic cancer cells, which carry a homologous deletion of the *CDKN2A* locus [37] and thus lack both p16 and p14 expression (Figure 7A). AsPC-1 cells express p53 from an allele that carries a single nucleotide deletion (TGC→GC) at Cys135 that produces a frameshift [37]. Hence, these cells express a truncated and dysfunctional p53 protein, which is also unstable, and are thus devoid of p21 expression (Figure 7B). Subsequently, we tested the effect of PR55 α -knockdown on senescence induction by IR in AsPC-1 cells using the SA- β -galactosidase assay. As shown in Figures 7B, 7C, IR exposure of AsPC-1 cells did not lead to senescence induction either in the presence or absence of the PR55 α knockdown by shRNA. These results, together with the data obtained from CD18/HPAF cells, which also express mutant p53 but possess a functional p16 (Figures 2B and 6B), suggest a role for PR55 α in the inhibition of the p16/RB pathway-dependent senescence induction by IR.

PR55 α expression inversely correlates with the expression of p16 in normal human tissues

We analyzed the co-expression of PR55 α and p16 in serial sections of human normal tissue specimens derived from various organs (bladder, colon, fallopian tube, heart, lung, liver, kidney, pancreas, and skin). Since p16 expression increases as a function of age, we subdivided specimens into two cohorts based on the donor's age: a "young" cohort consisting of tissues derived from individuals younger than 43 years old (y/o) and an "old" cohort consisting of the tissues derived from individuals

older than 68 y/o. As shown in Figure 8, there was a statistically significant inverse correlation between PR55 α and p16 expression in both young and old cohorts of tissues, with PR55 α levels detected at higher levels in tissues of young donors compared to old donors and p16 levels exhibiting the opposite relationship. Indeed, PR55 α levels were significantly lower in the old cohort compared to the young cohort. Conversely, the p16 levels were significantly higher in the old cohort compared to the young cohort.

DISCUSSION

Cellular senescence, both replicative and stress-induced, relies on the p16/RB and/or p53/p21 pathways to inhibit the G1 CDKs to block the cell cycle at the G1/S border [42, 43, 63–65]. Acting as a major obstacle to oncogenesis, senescence is induced in response to various genotoxic stimuli, such as telomere uncapping,

DNA damage, oxidative stress, and oncogene activation [66]. Consequently, the loss of function mutations in p53 and p16 tumor suppressors are the most frequent genetic alterations detected in human cancers [12, 45, 67]. In pancreatic cancer, the incidence of mutations affecting p53 and p16 function has been reported at 60–70% and 30–50% of all cases, respectively [40]. We previously reported on the essential role played by PR55 α -controlled PP2A in the activation of oncogenic pathways involving ERK, YAP, β -catenin, and c-Myc, all of which are known to be essential for pancreatic cancer tumorigenesis and progression [23–26]. In this report, we present results that reveal a novel function of PR55 α in the inhibition of p16 mRNA expression and abrogation of IR-induced premature senescence, and this PR55 α function was observed in normal HPNE cells expressing ectopic PR55 α , as well as in CD18/HPAF cells with PR55 α silenced by shRNA (see Figures 2, 3, and 6). In normal HPNE cells, while

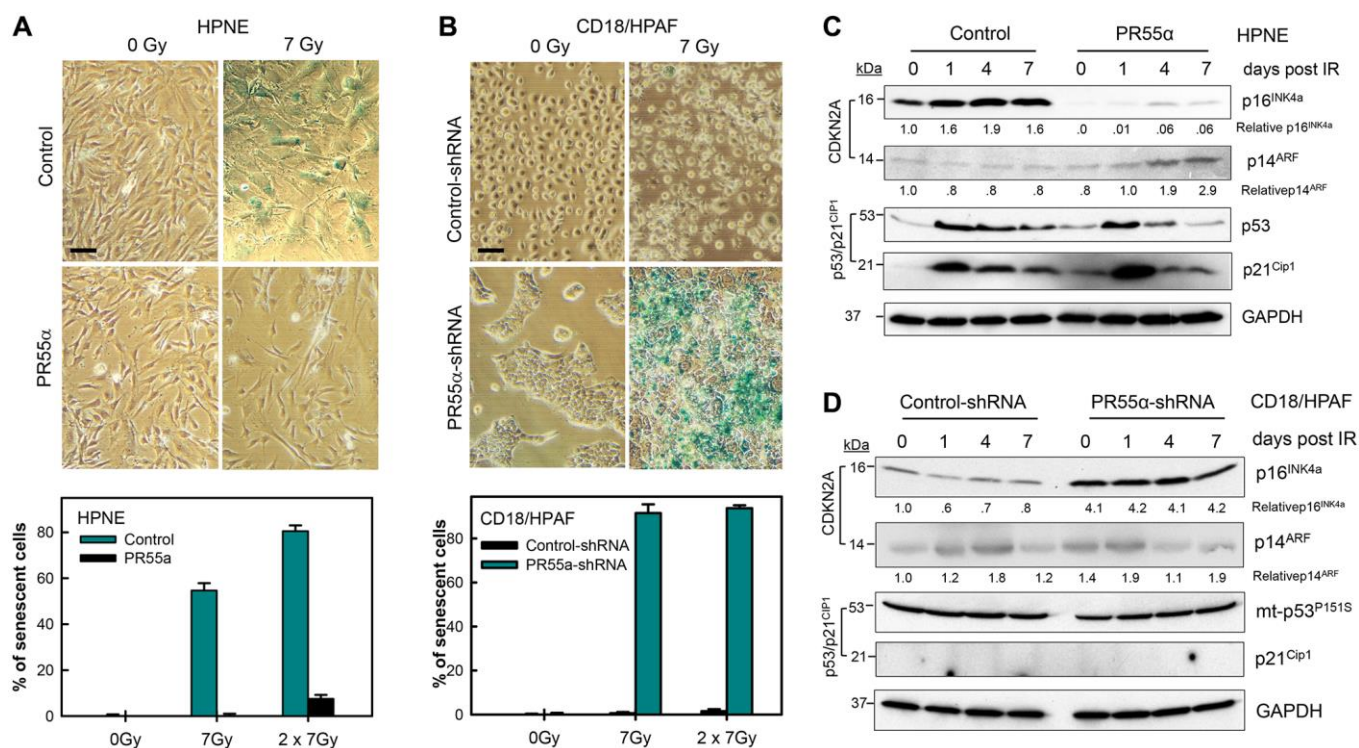


Figure 6. PR55 α inhibits IR-induced cellular senescence. (A) Ectopic PR55 α overexpression prevents senescence induction by IR in normal HPNE cells. HPNE/PR55 α and HPNE/control cells were incubated in the presence of 1 μ g/ml Dox for 2 days (to induce ectopic PR55 α in the HPNE/PR55 α cells) and then exposed to 7 Gy IR or left unirradiated as control (0 Gy). When the second radiation dose was applied, the interval was 24 hours between the two doses. Seven days post-IR, cells were assessed for SA- β -gal activity and photographed. Scale bar = 1 μ m. The bar graph expresses the percent of senescent cells in the indicated samples and represents the mean \pm S.D. of two separate experiments with each one in duplicate samples. (B) PR55 α -knockdown sensitizes CD18/HPAF pancreatic cancer cells to senescence induction by IR. CD18/HPAF cells expressing Dox-inducible PR55 α -shRNA or Control-shRNA were cultivated in the presence of 2 μ g/ml Dox for 5 days, to allow time to silence PR55 α expression, and then exposed to 7 Gy IR, or left unirradiated as a control (0 Gy). After 7 days, the cells were assessed for SA- β -gal activity and photographed. Scale bar = 1 μ m. The graphs express the percent of senescent cells in the indicated samples and represent the mean \pm S.D. of two separate experiments with each one in duplicate samples. (C, D) Normal HPNE and CD18/HPAF pancreatic cancer cells, with/without PR55 α manipulation, were exposed to 7 Gy IR, or left unirradiated as a control (0 day). When the second radiation dose was applied, the interval was 24 hours between the two doses. The irradiated cells were incubated for the times indicated and analyzed by immunoblotting for the differences in levels of p16, p14, p53, and p21. GAPDH was used as an internal control.

ectopic PR55 α inhibited p16 expression and IR-induced senescence, it simultaneously caused activation of the p53/p21 cascade (see Figure 2A). This increase in p53/p21 signaling, which did not appear to be associated with an increase in p14 (see Figures 1, 2, and 6), could be part of a negative feedback loop auto-regulating PR55 α levels. In a recent article, we report that the protein stability of PR55 α is negatively regulated by p53 in conjunction with the E3 ubiquitin ligase FBXL20 [28]. Hence, when PR55 α is in excess, the activation of p53 could also increase the expression of the p53-regulated FBXL20 gene, thereby causing PR55 α degradation. A similar loop is known to operate between p53 and its

negative regulator, MDM2 [68]. Future studies will be needed to elucidate the nature of this possible auto-feedback regulatory mechanism.

A significant finding of the current study is the ability of PR55 α to block cellular senescence induced by IR in both normal and cancer cells (See Figure 6). Furthermore, this novel function of PR55 α is linked to its ability to inhibit the p16/RB pathway but not the p53/p21 pathway (see Figures 2 and 6), given the opposite effects of PR55 α on the two pathways and the fact that PR55 α regulates p16 and IR-induced senescence even in the absence of a functional p53/p21

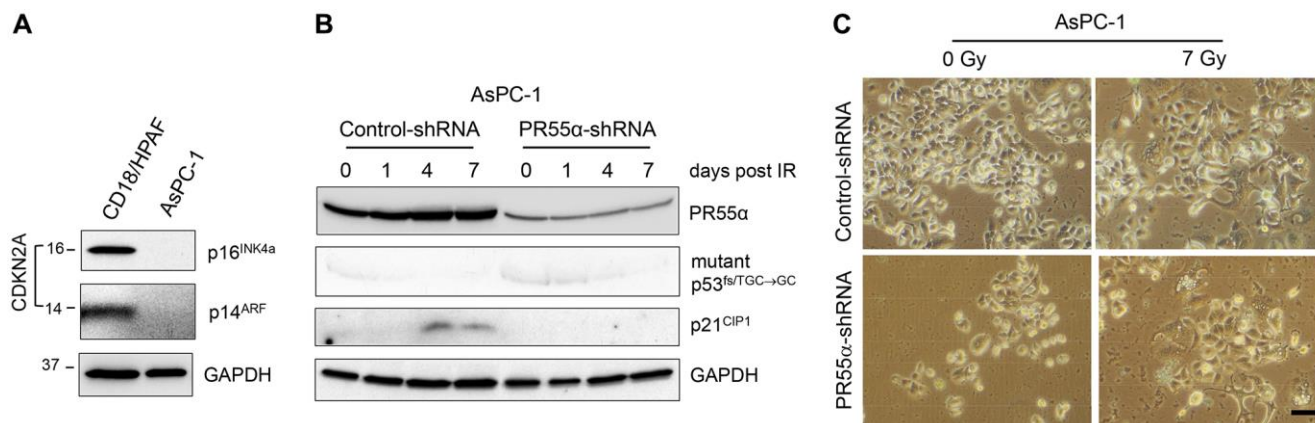


Figure 7. Knockdown of PR55 α does not result in senescence induction by IR in pancreatic cancer cells that lack p16 expression. (A) The *CDKN2A* locus, which encodes the p16 and p14 genes, is deleted from AsPC-1 pancreatic cancer cells [37]. Log-phase growing AsPC-1 cells were analyzed for the presence of p16 and p14 proteins with CD18/HPAF pancreatic cancer cells as a positive control. (B) AsPC-1 cells stably transduced with the Dox-inducible PR55 α -shRNA or Control-shRNA were induced with 2 μ g/ml Dox for 3 days to knock down PR55 α . The cells were then exposed to 7 Gy IR, or left unirradiated (0 time point), and incubated for an additional 1, 4 and 7 days. The cells were analyzed by immunoblotting for the levels of PR55 α , p53, and p21. GAPDH level was measured as an internal loading control. (C) The irradiated cells incubated for 7 days were analyzed for senescence by SA- β -gal activity assay and photographed. Scale bar = 1 μ m.

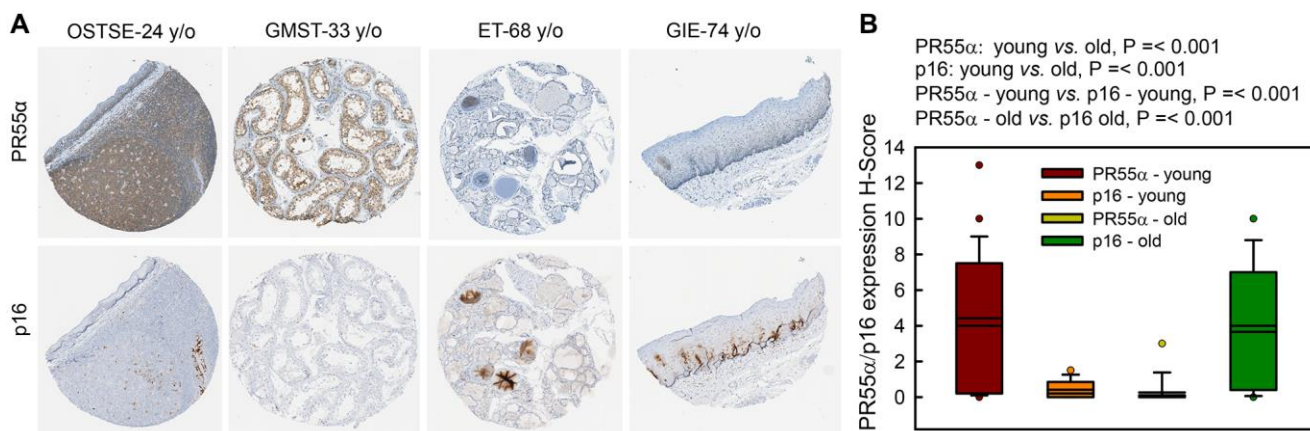


Figure 8. PR55 α level is much lower in human normal tissue specimens of older individuals compared to younger individuals and inversely correlates with p16 levels. Human normal tissue specimens derived from various organs/sites were analyzed for differences in PR55 α and p16 expression by IHC. (A) Representative images of adjacent tissue sections stained with anti-PR55 α and anti-p16 antibodies. OSTSE—tonsil; GMST—seminiferous tubules; ET—thyroid; GIE—esophagus. Young, ≤ 43 y/o; Old, ≥ 68 y/o; (B) Box plot shows the H-Score quantification of PR55 α and p16 expression from adjacent sections.

pathway, as in CD18/HPAF cells. Conversely, in AsPC-1 pancreatic cancer cells, which contain the p16 gene homologous deletion, silencing PR55 α did not result in senescence induction after IR (See Figure 7). We tested whether the re-introduction of p16 using an adenoviral vector (Ad.p16) could suffice to enable the senescence response to IR in AsPC-1 cells to allow testing the impacts of PR55 α . However, ectopic p16 expression in AsPC-1 cells instead resulted in apoptosis induction, as determined by visual inspection and detection of caspase 3 cleavage (data not shown). This p16-induced apoptosis has been reported before in breast cancer cells [69] and may be due to the dependence and addition of these cancer cells to their complete loss of endogenous p16. In summary, these results indicate that PR55 α blocks senescence by specifically inhibiting p16 expression and p16/RB signaling (Figure 1).

We have previously reported that the protein stability of PR55 α is negatively regulated by the p53/FBXL20 pathway [28]. We also have shown that PR55 α is necessary to activate several oncogenic pathways that promote pancreatic cancer, such as YAP, c-Myc, β -catenin, and ERK [23, 27, 28]. Consequently, by negatively regulating PR55 α protein stability, p53 can indirectly inhibit these oncogenic pathways and, at the same time, promote the induction of senescence by removing the inhibition of p16 expression exerted by PR55 α . Conversely, the loss of p53 function can result in the induction of PR55 α expression [28], which in turn can activate the same group of oncogenic pathways while suppressing the expression of p16 and induction of senescence. Future studies are needed to investigate whether PR55 α significantly contributes to the transcriptional suppression of p16 expression in some cancers that harbor mutant p53, such as pancreatic cancer, in which PR55 α is coincidentally overexpressed [27, 31, 70]. Likewise, when normal human cells become senescent, p53 becomes activated and p16 is induced [47, 71]. These events may also include the downregulation of PR55 α by the p53/FBXL20 axis, which could also contribute at least in part to the induction of p16 at senescence. This crosstalk between p53 and the p16/RB pathway enabled by PR55 α could potentially explain why in certain normal cells, the loss of p53 function is sufficient to overcome senescence, such as in mouse embryonic fibroblasts [72] or human mammary epithelial cells [73].

Current findings may also be extrapolated to senescence triggered by other genotoxic stressors, such as chemotherapeutic agents. Chemotherapy-induced senescence (CIS) is commonly observed after cancer treatments and is believed to contribute to tumor growth inhibition and cancer remission, whereas emerging evidence suggests that a small subset of tumor cells can escape CIS and lead to cancer recurrence [74, 75]. However, the

mechanisms responsible for the bypass of CIS are not well understood. In this report, we show that PR55 α overexpression can inhibit the p16/RB pathway and block senescence induction by IR. In future studies, we will determine if PR55 α can also block CIS and, in turn, cause chemoresistance in cancer patients.

In response to IR-induced DNA damage, ATM, ATR, and DNA-PK kinases are rapidly activated, which, in turn, induce their respective downstream effectors to activate cell cycle checkpoint responses, leading to cell cycle arrest and DNA repair [50]. However, when DNA damage cannot be repaired, apoptosis or senescence is triggered to eliminate the injured cells [50]. We have not observed evidence indicating that the DNA damage response regulates the level or activity of PR55 α -controlled PP2A. But because PR55 α inhibits p16 expression, it could instead influence the cells' decision to undergo cell cycle arrest, senesce, or apoptosis. Future studies will be needed to identify the impact of PR55 α on the fate of cellular response to DNA damage and evaluate the significance of this effect on the risk of oncogenic transformation.

During natural aging, there is a gradual accumulation of p16-expressing senescent cells in tissues [76]. To investigate the significance of PR55 α in this up-regulation of p16, we compared levels of the p16 and PR55 α proteins in a panel of normal tissue specimens derived from young (≤ 43 y/o) and old (≥ 68 y/o) donors. The results obtained are consistent with the notion that PR55 α negatively regulates p16 transcriptional expression, revealing a significant inverse correlation between p16 and PR55 α levels, in young tissues having PR55 α -high/p16-low and in older tissue having PR55 α -low/p16-high (Figure 8). These results are in line with the notion that PR55 α inhibits p16 expression (Figure 1). Future studies will be needed to understand the inter-relationships among p53, FBXL20, PR55 α , and p16 expression in human tissues following aging.

p16 expression is commonly regulated at the mRNA level [38]. A few mechanisms are reported to regulate p16, including changes in *CDKN2A* promoter methylation, epigenetic histone marks, altered transcription factors, and changes in the stability of p16 mRNA [77]. Our results indicate that the regulation of p16 expression by PR55 α also occurs at the p16 mRNA transcription level. This conclusion is based on our comprehensive analyses of the effects of PR55 α on p16 protein stability, p16 mRNA level, and p16 promoter activity (see Figures 3A–3C). Furthermore, since the AUF1 knockdown by siRNA did not prevent the negative regulation of p16 expression by PR55 α in HPNE cells (see Figure 3D), AUF1-mediated p16 mRNA decay is also not responsible for the inhibitory

effect of PR55 α on p16. The *CDKN2A* locus encodes for both p16 and p14 and the entire locus is subjected to epigenetic regulation by polycomb group protein complexes (PcG) and histone modifications (H3K27me3, H2AK119ub, H3K4me3), but the p16 and p14 promoters can still be differentially regulated by their respective transcription factors [78]. Our results show that PR55 α specifically reduces p16 expression, not that of p14. While we cannot exclude the possibility that PR55 α is also affecting the epigenetic regulators of p16 expression, PR55 α -controlled PP2A appears to directly regulate the p16 promoter in luciferase reporter assays (Figure 3). Further studies will be necessary to determine how PR55 α regulates p16 transcription and which transcription factors and epigenetic regulators are involved.

Both p53 and p16 are described as key regulators of senescence [1, 8, 43]. p16 inhibits the CDK4/6 kinases and the p53/p21 cascade blocks the CDK2 kinase, both of which result in RB activation and its sequestration of the E2F transcription factor, thus arresting the cell cycle in the G1 phase during senescence [79] (Figure 1). In this study, we assessed the effects of PR55 α on the induction of cellular senescence by IR both in normal cells expressing wt p53 (HPNE) and in cancer cells expressing mutant p53 (CD18/HPAF, AsPC-1). Among the three cell lines, only in AsPC-1 cells IR failed to induce senescence (Figure 7) in either the parental control cells (PR55 α -high) or PR55 α -shRNA knockdown cells (PR55 α -low). The main difference among the three cell lines is in the mutational status of their p16 gene. The locus is intact in HPNE cells but is homozygously deleted in the AsPC-1 cells [37, 54] (Figure 7A). In the CD18/HPAF cells, the p16 protein carries an in-frame deletion (aa 29–34) but is still reportedly functional [37, 54]. Our results support the notion that this p16 protein still has retained its ability to induce senescence in response to IR, as its up-regulation by the PR55 α knockdown is associated with IR-induced senescence (Figure 6B, 6D). This situation may also apply to other pancreatic cancer cell lines expressing p16 mutants, which may still be biologically functional for inducing cellular senescence. Nonetheless, the current studies cannot exclude the possibility that PR55 α may also affect other key regulators of senescence in addition to its inhibition of p16 expression. However, the study of this possibility is beyond the scope of the current investigation.

In summary, the results from this study reveal a novel function of PR55 α -controlled PP2A Ser/Thr phosphatase complexes in the inhibition of IR-induced senescence, which involves its inhibition of the p16/RB pathway that inhibits E2F activity to block the cell cycle. Future studies will be needed to identify the

precise molecular targets of PR55 α within the epigenetic and transcriptional regulators of p16 expression. Together, the results of this report establish PR55 α -controlled PP2A phosphatase as a critical new regulator of p16 expression and IR-induced senescence. Future studies will need to delineate the interplays among PR55 α , p53, and p16 in the maintenance of cellular homeostasis or induction of cellular senescence, as well as how the dysregulation of these pathways promotes cancer or aging.

MATERIALS AND METHODS

Cell culture and treatment

The HPNE cells are primary human pancreatic normal ductal cells immortalized with human telomerase hTERT [32, 33]. The Doxycycline (Dox)-inducible HPNE-PR55 α cell line was established by transducing HPNE cells with the pRevTet-On retroviral vector (Clontech Laboratories, Mountain View, CA, USA) modified to express the PR55 α cDNA and selecting the cells with hygromycin 200 μ g/ml. The ectopic expression of PR55 α was induced by 1 μ g/ml Dox for 48–72 h. The HPNE isogenic cell lines were maintained in Medium D growth medium (3 parts high glucose Dulbecco's modified Eagle's medium (DMEM) (GE Healthcare Life Sciences, Pittsburgh, PA, USA) to one part of M3 medium (INCELL, San Antonio, TX, USA) supplemented with 10% Tet-free FBS and 10 ng/mL human recombinant EGF (Invitrogen, Waltham, MA, USA)) [32, 33]. Human pancreatic cancer cell lines CD18/HPAF and AsPC-1 were obtained from ATCC (Manassas, VA, USA) and maintained in DMEM (Life Technologies, Carlsbad, CA, USA) with 10% fetal bovine serum (FBS) in an atmosphere containing 5% CO₂. IR exposure was performed by treating exponentially growing cells with a Mark I 68A Cesium-137 Irradiator (JL Shepherd and Associates, San Fernando, CA, USA) at the indicated doses and incubated for the specified times at 37°C.

Antibodies, Western blot analysis, and protein stability assessment

The primary antibodies used in this study were mouse IgG against p16 (#55079, BD Bioscience, USA), GAPDH (#32233, Santa Cruz, USA), and AUF1 (#12382, Cell Signaling Technologies, USA). Western blot analyses were performed as described previously [23, 28]. In brief, protein samples were separated by SDS-PAGE and transferred to a nitrocellulose membrane. The membrane was then probed with the primary antibody against p16, AUF1, or GAPDH, followed by detection using an anti-mouse IgG secondary antibody conjugated to horseradish

peroxidase. Chemiluminescent signals were captured and analyzed with a BioRad Chemidoc System (Hercules, CA, USA). Alternatively, they were revealed after exposure to an x-ray film and scanning of the film with an EPSON Perfection 4490 PHOTO scanner. Signal quantitation was done using the Fiji-ImageJ analytical program (NIH, Bethesda, MD, USA).

To analyze the protein half-life of p16, we exposed cells to protein synthesis inhibitor cycloheximide (CHX, dissolved in water) (Sigma-Aldrich, St. Louis, MO, USA) at 15 µg/ml and we began monitoring the levels of p16 protein by immunoblotting, as described previously [23, 28]. α -Tubulin served as a loading control on the Western blots. The levels of p16 on the blot were normalized by control protein levels, and calculated for half-life times ($t(1/2)$) by linear regression analysis of log (protein level) against time using the SigmaPlot graphing and data analysis software, as described in our studies [23, 28].

Senescence-associated β -galactosidase (SA- β -gal) assay

The SA- β -gal activity was measured per the manufacturer's instructions (Catalog #200488, Agilent Technologies, La Jolla, CA, USA). The SA- β -gal activity was determined by using X-gal (5-bromo-4-chloro-3-indolyl β -D-galactosidase) staining at pH 6.0. Ten randomly selected fields per sample were photographed and quantified for the cells positive in SA- β -gal staining under a light microscope.

Cell cycle analysis

Cell cycle analysis was carried out as described previously [80, 81]. Briefly, 24 h after IR exposure, the cells were harvested, washed with phosphate-buffered saline (PBS), and fixed in ice-cold ethanol. Cells were stained with propidium iodide (PI) and analyzed for DNA content by fluorescence-activated cell sorting (FACS) analysis using the FACS Calibur instrument (Becton Dickinson, Mansfield, MA, USA). At least 20,000 cells from each sample were evaluated.

Luciferase reporter constructs and luciferase assay

pGL2-p16-Luc is a firefly luciferase reporter for p16 promoter activity. It carries a firefly luciferase gene under the control of the p16 promoter (from nucleotides -3243 to -165 upstream of the p16 initiation codon). p16 promoter sequences were initially amplified by PCR using primers p16A (5'-cggatataccgctccacccaaggatgccataat-3'; MluI site underlined) and p16B (5'-ctgaagatctcccgccgcccggctccat-3'; BglIII site underlined). The PCR product was digested with MluI and BglIII and inserted into the

same sites of the pGL2-Basic vector (Promega, Madison, WI, USA). Next, this plasmid was digested with SacII and BglIII and then self-ligated to eliminate the segment -164 to +17 containing the p16 initiation codon. pRL-SV40-Luc (Promega) is a control Renilla luciferase reporter that contains the SV40 promoter. pGL2-p16-Luc and pRL-SV40-Luc were co-transfected into the cells using Lipofectamine 2000 (Invitrogen, Waltham, MA, USA) according to the manufacturer's suggestions. Firefly luciferase and Renilla luciferase activities were measured at 48 h following transfections using a Luciferase Assay System, as instructed by the manufacturer (Promega). Firefly luciferase activity was normalized for transfection efficiency using the activity of Renilla luciferase.

RNA isolation and real-time quantitative reverse transcription (qRT)-PCR

RNA was isolated from cells using TRIzol and reverse transcribed using the iScript Reverse Transcription kit. Further, the mRNA was quantified by Real-Time qRT-PCR using SsoAdvanced TM SYBR Green Supermix (Bio-Rad) following the manufacturer's protocols. GAPDH was used as the internal control. The following primers were used for the PCR: p16 forward primer: 5'-GACCTGGCTGAGGAGCTG-3' and p16 reverse primer: 5'-CAATCGGGGATGTCTGAGGG-3'; GAPDH forward primer: 5'-TTCCACCCATGGCAAATTCC-3' and reverse primer: 5'-TGGCAGGTTTTTCTAGACGG-3'.

Small hairpin RNAs, short interfering RNAs, and transfection

The small hairpin RNAs (shRNA) sequences targeting human PR55 α (PPP2R2A) mRNA are 5'-ATGGCTAGCAGACATGGAG-3', and 5'-CAACTATCTCAACTAAGCA-3'. The non-targeting control shRNA was designed to target no known genes in humans, mice, or rats. The control shRNA sequence is 5'-ATCTCGCTTGGGCGAGAGTAAG-3' (Dharmacon, Lafayette, CO, USA). The siGENOME/AUF1 short interfering RNAs (siRNAs) SMARTpool (Dharmacon) consists of four siRNAs targeting multiple sites on AUF1 mRNA: 5'-CAAAUUUGGUGAAGUUGUA-3', 5'-GGAAGGUGAUUGAUCCUAA-3', 5'-AGACUGCACUCUGAAGUUA-3', and 5'-CGUGGGUUCUGCUUUAUUA-3'. Control siGENOME nontargeting siRNA (Dharmacon) was designed to target no known genes in humans, mice, or rats. The sequence of the control siRNA is 5'-UAGCGACUAAACACAUCAA-3'. siRNA transfection of cells was performed with DharmaFECT-1 (Thermo Fisher Scientific, Waltham, MA, USA) as instructed by the manufacturer. Transfected cells were incubated for 48–72 hours before analysis.

Human normal tissue specimens and immunohistochemistry

Human normal tissue samples (CHTN_Norm3 - Normal Tissue Survey) for immunohistochemistry (IHC) analyses were provided by the Cooperative Human Tissue Network (Mid-Atlantic Division) funded by the National Cancer Institute. The normal tissue samples were derived from various human organs/sites including the skin, bladder, breast, digestive tracts, heart, kidney, liver, ovary, pancreas, spleen, and tonsil of both young (≤ 43 years old) and old (≥ 68 years old) individuals (Supplementary Table 1). The IHC analysis of PR55 α used the anti-PR55 α antibody 100C1 (Cell Signaling Technology, Danvers, MA, USA) at the dilution of 1:400. The IHC analysis of p16 used the anti-p16 JC2 mouse monoclonal IgG (ready use, MM156-10, Statlab, USA). The IHC analyses were performed by the Tissue Science Core of the University of Nebraska Medical Center (UNMC). PR55 α and p16 IHC staining were evaluated by a UNMC pathologist who was blinded to the clinical information. Immunohistochemistry (IHC) staining was quantified by a Histoscore (H-score) based on both signal intensity (0 = no staining, 1 = weak, 2 = moderate, 3 = strong immunoreactivity) and percentage of positive cells (1 = 0–25%, 2 = 26–50%, 3 = 51–75%, 4 = 76–100%), as we have done in previous studies [27, 28, 82].

Statistical analysis

Student's *t*-test and one-way ANOVA methods were used to compare experimental groups using SigmaPlot software (Palo Alto, CA, USA), and the results were expressed as mean \pm SD. The statistical analyses were described in the respective figure legends and *P*-values ≤ 0.05 were considered significant.

AUTHOR CONTRIBUTIONS

CP performed experiments, analyzed data, and participated in manuscript preparation. LSVM performed experiments and analyzed data. ALH constructed Dox-inducible cell lines and scored IHC-stained samples. CBJ performed experiments and reviewed the manuscript. BTG provided technical assistance and reviewed the manuscript. ALC assisted with studies and reviewed the manuscript. SZ provided technological support and reviewed the manuscript. CAE provided valuable discussions on the studies and reviewed the manuscript. MMO participated in the design of studies and provided critical discussion and revision of the manuscript. YY designed and supervised the studies, analyzed the data, and wrote the manuscript.

ACKNOWLEDGMENTS

We thank James Talaska for assistance with the confocal microscopes of the UNMC Microscopy Core Facility (a facility supported by the grant P30GM106397) and Victoria Smith for assistance with FACS analysis of the cell cycle.

CONFLICTS OF INTEREST

The authors declare no conflicts of interest related to this study.

FUNDING

This work was supported, in part, by NIH/NIGMS/R01GM143329 (to YY), NIH/NCI/R01CA206444 (to MMO), U.S. Army/USAMRAA/CDMRP/W81XWH-21-1-0700 (to YY), Nebraska/DHHS (2022-59) (to YY), University of Nebraska Collaboration Initiative Program Award (to YY and SZ), and a pilot project award (to YY and SZ) from the Great Plains IDeA-CTR-Program (NIH/NIGMS/5U54GM115458).

REFERENCES

1. Chen J, Huang X, Halicka D, Brodsky S, Avram A, Eskander J, Bloomgarden NA, Darzynkiewicz Z, Goligorsky MS. Contribution of p16INK4a and p21CIP1 pathways to induction of premature senescence of human endothelial cells: permissive role of p53. *Am J Physiol Heart Circ Physiol*. 2006; 290:H1575–86.
<https://doi.org/10.1152/ajpheart.00364.2005>
PMID:[16243918](https://pubmed.ncbi.nlm.nih.gov/16243918/)
2. Kim JY, Atanassov I, Dethloff F, Kroczeck L, Langer T. Time-resolved proteomic analyses of senescence highlight metabolic rewiring of mitochondria. *Life Sci Alliance*. 2023; 6:e202302127.
<https://doi.org/10.26508/lsa.202302127>
PMID:[37321846](https://pubmed.ncbi.nlm.nih.gov/37321846/)
3. Lee BY, Han JA, Im JS, Morrone A, Johung K, Goodwin EC, Kleijer WJ, DiMaio D, Hwang ES. Senescence-associated beta-galactosidase is lysosomal beta-galactosidase. *Aging Cell*. 2006; 5:187–95.
<https://doi.org/10.1111/j.1474-9726.2006.00199.x>
PMID:[16626397](https://pubmed.ncbi.nlm.nih.gov/16626397/)
4. Mirzayans R, Andrais B, Scott A, Murray D. New insights into p53 signaling and cancer cell response to DNA damage: implications for cancer therapy. *J Biomed Biotechnol*. 2012; 2012:170325.
<https://doi.org/10.1155/2012/170325>
PMID:[22911014](https://pubmed.ncbi.nlm.nih.gov/22911014/)

5. Mirzayans R, Andrais B, Hansen G, Murray D. Role of p16(INK4A) in Replicative Senescence and DNA Damage-Induced Premature Senescence in p53-Deficient Human Cells. *Biochem Res Int.* 2012; 2012:951574.
<https://doi.org/10.1155/2012/951574>
PMID:[22924132](https://pubmed.ncbi.nlm.nih.gov/22924132/)
6. Kim JH, Brown SL, Gordon MN. Radiation-induced senescence: therapeutic opportunities. *Radiat Oncol.* 2023; 18:10.
<https://doi.org/10.1186/s13014-022-02184-2>
PMID:[36639774](https://pubmed.ncbi.nlm.nih.gov/36639774/)
7. Blomen VA, Boonstra J. Cell fate determination during G1 phase progression. *Cell Mol Life Sci.* 2007; 64:3084–104.
<https://doi.org/10.1007/s00018-007-7271-z>
PMID:[17891333](https://pubmed.ncbi.nlm.nih.gov/17891333/)
8. Mijit M, Caracciolo V, Melillo A, Amicarelli F, Giordano A. Role of p53 in the Regulation of Cellular Senescence. *Biomolecules.* 2020; 10:420.
<https://doi.org/10.3390/biom10030420>
PMID:[32182711](https://pubmed.ncbi.nlm.nih.gov/32182711/)
9. Prieur A, Besnard E, Babled A, Lemaitre JM. p53 and p16(INK4A) independent induction of senescence by chromatin-dependent alteration of S-phase progression. *Nat Commun.* 2011; 2:473.
<https://doi.org/10.1038/ncomms1473>
PMID:[21915115](https://pubmed.ncbi.nlm.nih.gov/21915115/)
10. Beckerman R, Prives C. Transcriptional regulation by p53. *Cold Spring Harb Perspect Biol.* 2010; 2:a000935.
<https://doi.org/10.1101/cshperspect.a000935>
PMID:[20679336](https://pubmed.ncbi.nlm.nih.gov/20679336/)
11. Kotake Y, Naemura M, Murasaki C, Inoue Y, Okamoto H. Transcriptional Regulation of the p16 Tumor Suppressor Gene. *Anticancer Res.* 2015; 35:4397–401.
PMID:[26168478](https://pubmed.ncbi.nlm.nih.gov/26168478/)
12. Serrano M. The tumor suppressor protein p16INK4a. *Exp Cell Res.* 1997; 237:7–13.
<https://doi.org/10.1006/excr.1997.3824>
PMID:[9417860](https://pubmed.ncbi.nlm.nih.gov/9417860/)
13. Wang W, Martindale JL, Yang X, Chrest FJ, Gorospe M. Increased stability of the p16 mRNA with replicative senescence. *EMBO Rep.* 2005; 6:158–64.
<https://doi.org/10.1038/sj.embor.7400346>
PMID:[15678155](https://pubmed.ncbi.nlm.nih.gov/15678155/)
14. White EJ, Matsangos AE, Wilson GM. AUF1 regulation of coding and noncoding RNA. *Wiley Interdiscip Rev RNA.* 2017; 8:e1393.
<https://doi.org/10.1002/wrna.1393>
PMID:[27620010](https://pubmed.ncbi.nlm.nih.gov/27620010/)
15. White EJ, Brewer G, Wilson GM. Post-transcriptional control of gene expression by AUF1: mechanisms, physiological targets, and regulation. *Biochim Biophys Acta.* 2013; 1829:680–8.
<https://doi.org/10.1016/j.bbagr.2012.12.002>
PMID:[23246978](https://pubmed.ncbi.nlm.nih.gov/23246978/)
16. Guo GE, Ma LW, Jiang B, Yi J, Tong TJ, Wang WG. Hydrogen peroxide induces p16(INK4a) through an AUF1-dependent manner. *J Cell Biochem.* 2010; 109:1000–5.
<https://doi.org/10.1002/jcb.22474>
PMID:[20069554](https://pubmed.ncbi.nlm.nih.gov/20069554/)
17. Brown VL, Harwood CA, Crook T, Cronin JG, Kelsell DP, Proby CM. p16INK4a and p14ARF tumor suppressor genes are commonly inactivated in cutaneous squamous cell carcinoma. *J Invest Dermatol.* 2004; 122:1284–92.
<https://doi.org/10.1111/j.0022-202X.2004.22501.x>
PMID:[15140233](https://pubmed.ncbi.nlm.nih.gov/15140233/)
18. Sherr CJ, McCormick F. The RB and p53 pathways in cancer. *Cancer Cell.* 2002; 2:103–12.
[https://doi.org/10.1016/s1535-6108\(02\)00102-2](https://doi.org/10.1016/s1535-6108(02)00102-2)
PMID:[12204530](https://pubmed.ncbi.nlm.nih.gov/12204530/)
19. Bates S, Phillips AC, Clark PA, Stott F, Peters G, Ludwig RL, Vousden KH. p14ARF links the tumour suppressors RB and p53. *Nature.* 1998; 395:124–5.
<https://doi.org/10.1038/25867>
PMID:[9744267](https://pubmed.ncbi.nlm.nih.gov/9744267/)
20. Shi Y. Serine/threonine phosphatases: mechanism through structure. *Cell.* 2009; 139:468–84.
<https://doi.org/10.1016/j.cell.2009.10.006>
PMID:[19879837](https://pubmed.ncbi.nlm.nih.gov/19879837/)
21. Reinhout S, Janssens V. Physiologic functions of PP2A: Lessons from genetically modified mice. *Biochim Biophys Acta Mol Cell Res.* 2019; 1866:31–50.
<https://doi.org/10.1016/j.bbamcr.2018.07.010>
PMID:[30030003](https://pubmed.ncbi.nlm.nih.gov/30030003/)
22. Amin P, Awal S, Vigneron S, Roque S, Mechali F, Labbé JC, Lorca T, Castro A. PP2A-B55: substrates and regulators in the control of cellular functions. *Oncogene.* 2022; 41:1–14.
<https://doi.org/10.1038/s41388-021-02068-x>
PMID:[34686773](https://pubmed.ncbi.nlm.nih.gov/34686773/)
23. Hein AL, Brandquist ND, Ouellette CY, Seshacharyulu P, Enke CA, Ouellette MM, Batra SK, Yan Y. PR55 α regulatory subunit of PP2A inhibits the MOB1/LATS cascade and activates YAP in pancreatic cancer cells. *Oncogenesis.* 2019; 8:63.
<https://doi.org/10.1038/s41389-019-0172-9>
PMID:[31659153](https://pubmed.ncbi.nlm.nih.gov/31659153/)

24. Adams DG, Coffee RL Jr, Zhang H, Pelech S, Strack S, Wadzinski BE. Positive regulation of Raf1-MEK1/2-ERK1/2 signaling by protein serine/threonine phosphatase 2A holoenzymes. *J Biol Chem.* 2005; 280:42644–54. <https://doi.org/10.1074/jbc.M502464200> PMID:16239230
25. Zhang L, Zhou H, Li X, Vartuli RL, Rowse M, Xing Y, Rudra P, Ghosh D, Zhao R, Ford HL. Eya3 partners with PP2A to induce c-Myc stabilization and tumor progression. *Nat Commun.* 2018; 9:1047. <https://doi.org/10.1038/s41467-018-03327-4> PMID:29535359
26. Zhang W, Yang J, Liu Y, Chen X, Yu T, Jia J, Liu C. PR55 alpha, a regulatory subunit of PP2A, specifically regulates PP2A-mediated beta-catenin dephosphorylation. *J Biol Chem.* 2009; 284:22649–56. <https://doi.org/10.1074/jbc.M109.013698> PMID:19556239
27. Hein AL, Seshacharyulu P, Rachagani S, Sheinin YM, Ouellette MM, Ponnusamy MP, Mumby MC, Batra SK, Yan Y. PR55 α Subunit of Protein Phosphatase 2A Supports the Tumorigenic and Metastatic Potential of Pancreatic Cancer Cells by Sustaining Hyperactive Oncogenic Signaling. *Cancer Res.* 2016; 76:2243–53. <https://doi.org/10.1158/0008-5472.CAN-15-2119> PMID:26893480
28. Madduri LSV, Brandquist ND, Palanivel C, Talmon GA, Baine MJ, Zhou S, Enke CA, Johnson KR, Ouellette MM, Yan Y. p53/FBXL20 axis negatively regulates the protein stability of PR55 α , a regulatory subunit of PP2A Ser/Thr phosphatase. *Neoplasia.* 2021; 23:1192–203. <https://doi.org/10.1016/j.neo.2021.10.002> PMID:34731788
29. Xiao J, Zhang T, Xu D, Wang H, Cai Y, Jin T, Liu M, Jin M, Wu K, Yuan J. FBXL20-mediated Vps34 ubiquitination as a p53 controlled checkpoint in regulating autophagy and receptor degradation. *Genes Dev.* 2015; 29:184–96. <https://doi.org/10.1101/gad.252528.114> PMID:25593308
30. Childs BG, Baker DJ, Kirkland JL, Campisi J, van Deursen JM. Senescence and apoptosis: dueling or complementary cell fates? *EMBO Rep.* 2014; 15:1139–53. <https://doi.org/10.15252/embr.201439245> PMID:25312810
31. Bardeesy N, Aguirre AJ, Chu GC, Cheng KH, Lopez LV, Hezel AF, Feng B, Brennan C, Weissleder R, Mahmood U, Hanahan D, Redston MS, Chin L, Depinho RA. Both p16(Ink4a) and the p19(Arf)-p53 pathway constrain progression of pancreatic adenocarcinoma in the mouse. *Proc Natl Acad Sci U S A.* 2006; 103:5947–52. <https://doi.org/10.1073/pnas.0601273103> PMID:16585505
32. Lee KM, Choi KH, Ouellette MM. Use of exogenous hTERT to immortalize primary human cells. *Cytotechnology.* 2004; 45:33–8. <https://doi.org/10.1007/10.1007/s10616-004-5123-3> PMID:19003241
33. Lee KM, Yasuda H, Hollingsworth MA, Ouellette MM. Notch 2-positive progenitors with the intrinsic ability to give rise to pancreatic ductal cells. *Lab Invest.* 2005; 85:1003–12. <https://doi.org/10.1038/labinvest.3700298> PMID:15924149
34. Berrozpe G, Schaeffer J, Peinado MA, Real FX, Perucho M. Comparative analysis of mutations in the p53 and K-ras genes in pancreatic cancer. *Int J Cancer.* 1994; 58:185–91. <https://doi.org/10.1002/ijc.2910580207> PMID:8026879
35. Arcangeli S, Greco C. Hypofractionated radiotherapy for organ-confined prostate cancer: is less more? *Nat Rev Urol.* 2016; 13:400–8. <https://doi.org/10.1038/nrurol.2016.106> PMID:27296648
36. Liu J, Lee P, McGee HM, Chung V, Melstrom L, Singh G, Raouf M, Amini A, Chen YJ, Williams TM. Advances in Radiation Oncology for Pancreatic Cancer: An Updated Review. *Cancers (Basel).* 2022; 14:5725. <https://doi.org/10.3390/cancers14235725> PMID:36497207
37. Moore PS, Sipos B, Orlandini S, Sorio C, Real FX, Lemoine NR, Gress T, Bassi C, Klöppel G, Kalthoff H, Ungefroren H, Löhner M, Scarpa A. Genetic profile of 22 pancreatic carcinoma cell lines. Analysis of K-ras, p53, p16 and DPC4/Smad4. *Virchows Arch.* 2001; 439:798–802. <https://doi.org/10.1007/s004280100474> PMID:11787853
38. Li J, Poi MJ, Tsai MD. Regulatory mechanisms of tumor suppressor P16(INK4A) and their relevance to cancer. *Biochemistry.* 2011; 50:5566–82. <https://doi.org/10.1021/bi200642e> PMID:21619050
39. Vaddavalli PL, Schumacher B. The p53 network: cellular and systemic DNA damage responses in cancer and aging. *Trends Genet.* 2022; 38:598–612. <https://doi.org/10.1016/j.tig.2022.02.010> PMID:35346511
40. Hu HF, Ye Z, Qin Y, Xu XW, Yu XJ, Zhuo QF, Ji SR. Mutations in key driver genes of pancreatic cancer:

- molecularly targeted therapies and other clinical implications. *Acta Pharmacol Sin.* 2021; 42:1725–41.
<https://doi.org/10.1038/s41401-020-00584-2>
PMID:33574569
41. Kasthuber ER, Lowe SW. Putting p53 in Context. *Cell.* 2017; 170:1062–78.
<https://doi.org/10.1016/j.cell.2017.08.028>
PMID:28886379
42. Shay JW, Wright WE. Senescence and immortalization: role of telomeres and telomerase. *Carcinogenesis.* 2005; 26:867–74.
<https://doi.org/10.1093/carcin/bgh296>
PMID:15471900
43. Takahashi A, Ohtani N, Hara E. Irreversibility of cellular senescence: dual roles of p16INK4a/Rb-pathway in cell cycle control. *Cell Div.* 2007; 2:10.
<https://doi.org/10.1186/1747-1028-2-10>
PMID:17343761
44. Roufayel R, Mezher R, Storey KB. The Role of Retinoblastoma Protein in Cell Cycle Regulation: An Updated Review. *Curr Mol Med.* 2021; 21:620–9.
<https://doi.org/10.2174/1566524020666210104113003>
PMID:33397238
45. Wagner KD, Wagner N. The Senescence Markers p16INK4A, p14ARF/p19ARF, and p21 in Organ Development and Homeostasis. *Cells.* 2022; 11:1966.
<https://doi.org/10.3390/cells11121966>
PMID:35741095
46. Rubin SM. Deciphering the retinoblastoma protein phosphorylation code. *Trends Biochem Sci.* 2013; 38:12–9.
<https://doi.org/10.1016/j.tibs.2012.10.007>
PMID:23218751
47. Safwan-Zaiter H, Wagner N, Wagner KD. P16INK4A-More Than a Senescence Marker. *Life (Basel).* 2022; 12:1332.
<https://doi.org/10.3390/life12091332>
PMID:36143369
48. Lundberg AS, Weinberg RA. Functional inactivation of the retinoblastoma protein requires sequential modification by at least two distinct cyclin-cdk complexes. *Mol Cell Biol.* 1998; 18:753–61.
<https://doi.org/10.1128/MCB.18.2.753>
PMID:9447971
49. Geng Y, Yu Q, Sicinska E, Das M, Bronson RT, Sicinski P. Deletion of the p27Kip1 gene restores normal development in cyclin D1-deficient mice. *Proc Natl Acad Sci U S A.* 2001; 98:194–9.
<https://doi.org/10.1073/pnas.98.1.194>
PMID:11134518
50. Ouellette MM, Zhou S, Yan Y. Cell Signaling Pathways That Promote Radioresistance of Cancer Cells. *Diagnostics (Basel).* 2022; 12:656.
<https://doi.org/10.3390/diagnostics12030656>
PMID:35328212
51. Wu Y, Song Y, Wang R, Wang T. Molecular mechanisms of tumor resistance to radiotherapy. *Mol Cancer.* 2023; 22:96.
<https://doi.org/10.1186/s12943-023-01801-2>
PMID:37322433
52. Ozaki T, Nakagawara A. Role of p53 in Cell Death and Human Cancers. *Cancers (Basel).* 2011; 3:994–1013.
<https://doi.org/10.3390/cancers3010994>
PMID:24212651
53. Smith HL, Southgate H, Tweddle DA, Curtin NJ. DNA damage checkpoint kinases in cancer. *Expert Rev Mol Med.* 2020; 22:e2.
<https://doi.org/10.1017/erm.2020.3>
PMID:32508294
54. Deer EL, González-Hernández J, Coursen JD, Shea JE, Ngatia J, Scaife CL, Firpo MA, Mulvihill SJ. Phenotype and genotype of pancreatic cancer cell lines. *Pancreas.* 2010; 39:425–35.
<https://doi.org/10.1097/MPA.0b013e3181c15963>
PMID:20418756
55. Chen T, Stephens PA, Middleton FK, Curtin NJ. Targeting the S and G2 checkpoint to treat cancer. *Drug Discov Today.* 2012; 17:194–202.
<https://doi.org/10.1016/j.drudis.2011.12.009>
PMID:22192883
56. Yan Y, Hein AL, Etekpó A, Burchett KM, Lin C, Enke CA, Batra SK, Cowan KH, Ouellette MM. Inhibition of RAC1 GTPase sensitizes pancreatic cancer cells to γ -irradiation. *Oncotarget.* 2014; 5:10251–70.
<https://doi.org/10.18632/oncotarget.2500>
PMID:25344910
57. Yan Y, Ouellette MM. Rac1 GTPase in pancreatic cancer. *Aging (Albany NY).* 2015; 7:609–10.
<https://doi.org/10.18632/aging.100804>
PMID:26420819
58. Vandenberk B, Brouwers B, Hatse S, Wildiers H. p16INK4a: A central player in cellular senescence and a promising aging biomarker in elderly cancer patients. *J Geriatr Oncol.* 2011; 2:259–69.
<https://doi.org/10.1016/j.jgo.2011.08.004>
59. Li P, Liu X, Zhao T, Li F, Wang Q, Zhang P, Hirayama R, Chen W, Jin X, Zheng X, Wang Z, Li Q. Comparable radiation sensitivity in p53 wild-type and p53 deficient tumor cells associated with different cell death modalities. *Cell Death Discov.* 2021; 7:184.
<https://doi.org/10.1038/s41420-021-00570-5>

- PMID:[34285189](#)
60. Rufini A, Tucci P, Celardo I, Melino G. Senescence and aging: the critical roles of p53. *Oncogene*. 2013; 32:5129–43.
<https://doi.org/10.1038/onc.2012.640>
PMID:[23416979](#)
61. Moulder DE, Hatoum D, Tay E, Lin Y, McGowan EM. The Roles of p53 in Mitochondrial Dynamics and Cancer Metabolism: The Pendulum between Survival and Death in Breast Cancer? *Cancers (Basel)*. 2018; 10:189.
<https://doi.org/10.3390/cancers10060189>
PMID:[29890631](#)
62. Dimri GP, Lee X, Basile G, Acosta M, Scott G, Roskelley C, Medrano EE, Linskens M, Rubelj I, Pereira-Smith O. A biomarker that identifies senescent human cells in culture and in aging skin in vivo. *Proc Natl Acad Sci U S A*. 1995; 92:9363–7.
<https://doi.org/10.1073/pnas.92.20.9363>
PMID:[7568133](#)
63. Roger L, Tomas F, Gire V. Mechanisms and Regulation of Cellular Senescence. *Int J Mol Sci*. 2021; 22:13173.
<https://doi.org/10.3390/ijms222313173>
PMID:[34884978](#)
64. Wiley CD, Campisi J. The metabolic roots of senescence: mechanisms and opportunities for intervention. *Nat Metab*. 2021; 3:1290–301.
<https://doi.org/10.1038/s42255-021-00483-8>
PMID:[34663974](#)
65. Bae I, Fan S, Bhatia K, Kohn KW, Fornace AJ Jr, O'Connor PM. Relationships between G1 arrest and stability of the p53 and p21Cip1/Waf1 proteins following gamma-irradiation of human lymphoma cells. *Cancer Res*. 1995; 55:2387–93.
PMID:[7757991](#)
66. Herbig U, Sedivy JM. Regulation of growth arrest in senescence: telomere damage is not the end of the story. *Mech Ageing Dev*. 2006; 127:16–24.
<https://doi.org/10.1016/j.mad.2005.09.002>
PMID:[16229875](#)
67. Liu Y, Chen C, Xu Z, Scuoppo C, Rillahan CD, Gao J, Spitzer B, Bosbach B, Kasthuber ER, Baslan T, Ackermann S, Cheng L, Wang Q, et al. Deletions linked to TP53 loss drive cancer through p53-independent mechanisms. *Nature*. 2016; 531:471–5.
<https://doi.org/10.1038/nature17157>
PMID:[26982726](#)
68. Zhao Y, Yu H, Hu W. The regulation of MDM2 oncogene and its impact on human cancers. *Acta Biochim Biophys Sin (Shanghai)*. 2014; 46:180–9.
<https://doi.org/10.1093/abbs/gmt147>
PMID:[24389645](#)
69. Kim M, Katayose Y, Rojanala L, Shah S, Sgagias M, Jang L, Jung YJ, Lee SH, Hwang SG, Cowan KH. Induction of apoptosis in p16INK4A mutant cell lines by adenovirus-mediated overexpression of p16INK4A protein. *Cell Death Differ*. 2000; 7:706–11.
<https://doi.org/10.1038/sj.cdd.4400703>
PMID:[10918444](#)
70. Azzopardi S, Pang S, Klimstra DS, Du YN. p53 and p16^{Ink4a}/p19^{Arf} Loss Promotes Different Pancreatic Tumor Types from PyMT-Expressing Progenitor Cells. *Neoplasia*. 2016; 18:610–7.
<https://doi.org/10.1016/j.neo.2016.08.003>
PMID:[27664376](#)
71. Kumari R, Jat P. Mechanisms of Cellular Senescence: Cell Cycle Arrest and Senescence Associated Secretory Phenotype. *Front Cell Dev Biol*. 2021; 9:645593.
<https://doi.org/10.3389/fcell.2021.645593>
PMID:[33855023](#)
72. Whibley C, Odell AF, Nedelko T, Balaburski G, Murphy M, Liu Z, Stevens L, Walker JH, Routledge M, Hollstein M. Wild-type and Hupki (human p53 knock-in) murine embryonic fibroblasts: p53/ARF pathway disruption in spontaneous escape from senescence. *J Biol Chem*. 2010; 285:11326–35.
<https://doi.org/10.1074/jbc.M109.064444>
PMID:[20118236](#)
73. Shay JW, Wright WE, Brasiskyte D, Van der Haegen BA. E6 of human papillomavirus type 16 can overcome the M1 stage of immortalization in human mammary epithelial cells but not in human fibroblasts. *Oncogene*. 1993; 8:1407–13.
PMID:[8389027](#)
74. Guillon J, Petit C, Toutain B, Guette C, Lelièvre E, Coqueret O. Chemotherapy-induced senescence, an adaptive mechanism driving resistance and tumor heterogeneity. *Cell Cycle*. 2019; 18:2385–97.
<https://doi.org/10.1080/15384101.2019.1652047>
PMID:[31397193](#)
75. Saleh T, Gewirtz DA. Considering therapy-induced senescence as a mechanism of tumour dormancy contributing to disease recurrence. *Br J Cancer*. 2022; 126:1363–5.
<https://doi.org/10.1038/s41416-022-01787-6>
PMID:[35304605](#)
76. Muss HB, Smitherman A, Wood WA, Nyrop K, Tuchman S, Randhawa PK, Entwistle AR, Mitin N, Shachar SS. p16 a biomarker of aging and tolerance for cancer therapy. *Transl Cancer Res*. 2020; 9:5732–42.
<https://doi.org/10.21037/tcr.2020.03.39>
PMID:[35117935](#)

77. Baylin SB, Jones PA. Epigenetic Determinants of Cancer. *Cold Spring Harb Perspect Biol.* 2016; 8:a019505.
<https://doi.org/10.1101/cshperspect.a019505>
PMID:[27194046](https://pubmed.ncbi.nlm.nih.gov/27194046/)
78. Laud K, Marian C, Avril MF, Barrois M, Chompret A, Goldstein AM, Tucker MA, Clark PA, Peters G, Chaudru V, Demenais F, Spatz A, Smith MW, et al, and French Hereditary Melanoma Study Group. Comprehensive analysis of CDKN2A (p16INK4A/p14ARF) and CDKN2B genes in 53 melanoma index cases considered to be at heightened risk of melanoma. *J Med Genet.* 2006; 43:39–47.
<https://doi.org/10.1136/jmg.2005.033498>
PMID:[15937071](https://pubmed.ncbi.nlm.nih.gov/15937071/)
79. Goel S, DeCristo MJ, McAllister SS, Zhao JJ. CDK4/6 Inhibition in Cancer: Beyond Cell Cycle Arrest. *Trends Cell Biol.* 2018; 28:911–25.
<https://doi.org/10.1016/j.tcb.2018.07.002>
PMID:[30061045](https://pubmed.ncbi.nlm.nih.gov/30061045/)
80. Yan Y, Black CP, Cao PT, Haferbier JL, Kolb RH, Spieker RS, Ristow AM, Cowan KH. Gamma-irradiation-induced DNA damage checkpoint activation involves feedback regulation between extracellular signal-regulated kinase 1/2 and BRCA1. *Cancer Res.* 2008; 68:5113–21.
<https://doi.org/10.1158/0008-5472.CAN-07-5818>
PMID:[18593910](https://pubmed.ncbi.nlm.nih.gov/18593910/)
81. Yan Y, Black CP, Cowan KH. Irradiation-induced G2/M checkpoint response requires ERK1/2 activation. *Oncogene.* 2007; 26:4689–98.
<https://doi.org/10.1038/sj.onc.1210268>
PMID:[17297454](https://pubmed.ncbi.nlm.nih.gov/17297454/)
82. Hein AL, Post CM, Sheinin YM, Lakshmanan I, Natarajan A, Enke CA, Batra SK, Ouellette MM, Yan Y. RAC1 GTPase promotes the survival of breast cancer cells in response to hyper-fractionated radiation treatment. *Oncogene.* 2016; 35:6319–29.
<https://doi.org/10.1038/onc.2016.163>
PMID:[27181206](https://pubmed.ncbi.nlm.nih.gov/27181206/)
83. Gorgoulis V, Adams PD, Alimonti A, Bennett DC, Bischof O, Bishop C, Campisi J, Collado M, Evangelou K, Ferbeyre G, Gil J, Hara E, Krizhanovsky V, et al. Cellular Senescence: Defining a Path Forward. *Cell.* 2019; 179:813–27.
<https://doi.org/10.1016/j.cell.2019.10.005>
PMID:[31675495](https://pubmed.ncbi.nlm.nih.gov/31675495/)
84. McHugh D, Gil J. Senescence and aging: Causes, consequences, and therapeutic avenues. *J Cell Biol.* 2018; 217:65–77.
<https://doi.org/10.1083/jcb.201708092>
PMID:[29114066](https://pubmed.ncbi.nlm.nih.gov/29114066/)

SUPPLEMENTARY MATERIALS

Supplementary Table

Supplementary Table 1. Human normal tissue samples from various organs/sites of young and old individuals were used to assess PR55 α and p16 protein expression by immunohistochemistry with H-score.

Case	Cohort	Tissue	Age	Gender	H-Score PR55 α	H-Score p16
1	Young	alveoli	1	Female	4.0	0.0
2	Young	alveoli	1	Female	0.2	0.0
3	Young	mucosa assoc. lymphoid tissue, appendix	6	Male	0.1	0.0
4	Young	mucosa assoc. lymphoid tissue, appendix	6	Male	0.1	0.0
5	Young	alveoli	1	Female	4.5	0.0
6	Young	thymus	19	Female	7.5	1.5
7	Young	thymus	19	Female	4.5	0.9
8	Young	thymus	19	Female	6.0	1.2
9	Young	skin, squamous epithelium	23	Female	0.1	0.2
10	Young	skin, squamous epithelium	23	Female	0.1	0.1
11	Young	skin, squamous epithelium	23	Female	0.2	0.1
12	Young	Breast, epithelium	23	Female	7.5	0.4
13	Young	Breast, epithelium	23	Female	8.0	0.8
14	Young	Breast, epithelium	23	Female	7.0	0.9
15	Young	tonsil, squamous epithelium	24	Female	7.0	0.4
16	Young	tonsil, squamous epithelium	24	Female	9.0	0.8
17	Young	kidney, cortex	25	Male	8.0	0.2
18	Young	kidney, medulla	25	Male	7.5	0.1
19	Young	kidney, medulla	25	Male	1.5	0.1
20	Young	ectocervix	26	Female	0.2	1.5
21	Young	Smooth muscle, uterus	28	Female	3.0	0.3
22	Young	Smooth muscle, uterus	28	Female	2.0	0.0
23	Young	Smooth muscle, uterus	28	Female	3.0	0.3
24	Young	Ovary, 1' oocytes	33	Female	9.0	0.3
25	Young	Ovary, 1' oocytes	33	Female	0.0	0.2
26	Young	Ovary, 1' oocytes	33	Female	0.2	0.2
27	Young	ovary, corpus luteum	33	Female	6.5	0.9
28	Young	ovary, corpus luteum	33	Female	7.5	1.5
29	Young	ovary, corpus luteum	33	Female	8.0	0.9
30	Young	endocervix	37	Female	1.0	0.0
31	Young	endocervix	37	Female	0.2	0.0
32	Young	amniotic membrane	39	Female	4.0	0.0
33	Young	amniotic membrane	39	Female	2.0	0.2
34	Young	amniotic membrane	39	Female	9.0	0.9
35	Young	fallopian tube	43	Female	10.0	0.3
36	Young	fallopian tube	43	Female	13.0	0.2
37	Young	fallopian tube	43	Female	2.0	0.0
38	Old	thyroid	68	Female	0.2	0.0
39	Old	thyroid	68	Female	0.0	0.1
40	Old	adrenal gland, cortex	71	Male	8.0	0.1
41	Old	adrenal gland, cortex	71	Male	8.0	0.0

42	Old	adrenal gland, medulla	71	Male	10.0	0.1
43	Old	adrenal gland, medulla	71	Male	7.0	0.1
44	Old	adrenal gland, medulla	71	Male	4.0	0.0
45	Old	esophagus, squamous mucosa	74	Female	4.5	0.1
46	Old	esophagus, squamous mucosa	74	Female	6.0	0.3
47	Old	esophagus, squamous mucosa	74	Female	5.0	3.0
48	Old	peripheral nerve	73	Female	0.4	0.1
49	Old	peripheral nerve	73	Female	0.4	0.0
50	Old	peripheral nerve	73	Female	0.4	0.0
51	Old	cartilage, articular	73	Female	0.8	0.0
52	Old	aorta, smooth muscle	85	Female	0.1	0.0

The "Young" cohort was ≤ 43 years old; the "Old" cohort was ≥ 68 years old.